Organic Photochemistry: From Fundamental Understanding to Functional Molecules and Novel Photoreactions

Habilitation Thesis

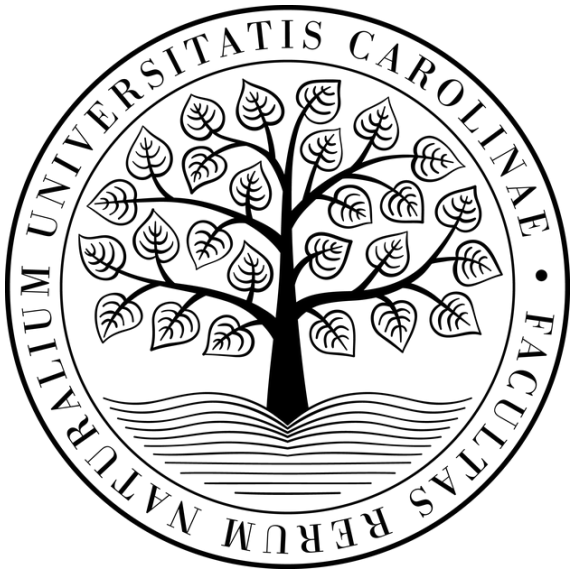

Tomáš Slanina

Faculty of Science

Charles University

2023

I would like to express my gratitude to my teachers, colleagues, collaborators, and students with whom I could share the passion for science and discover the beauty of chemistry. I am thankful to my family who support me in my scientific efforts and who are always patient, loving and nurturing.

List of Contents

Introduction

The interaction of *light* with *matter* has fascinated humans since the inception of science for light is ethereal, whereas matter is tangible. Yet, electromagnetic radiation absorption by molecules, which converts them into electronically excited states, explains how the universe was formed and the very essence of life on Earth. This scientific curiosity about visible and UV light interactions with molecules has led to the development of *photophysics*, the study of the radiative and non-radiative behaviour of molecular excited states, and *photochemistry*, the study of the chemical transformations induced by light. One field without the other would be incomplete because photophysics aims at understanding how molecular electron density responds to photon absorption and photochemistry seeks to rationalize how these changes in electron density distribution lead to the movement of chemical nuclei.

This habilitation thesis maps my efforts in the fields of photophysics and photochemistry of organic compounds to *understand the fundamental processes* that occur in excited closed- and open-shell molecules. In my research group, we have gained detailed insights into the electronic properties of these processes, which have enabled us to *design* various *functional molecular systems*, such as photocages and photoswitches, and new *photochemical reactions*, thereby achieving unique synthetic transformations.

This habilitation thesis consists of two sections – the first section describes organic chromophores, examining fundamental processes in their excited states and the design of functional molecules and systems. The second section focuses on open-shell molecules and addresses one more level of complexity – unpaired spin, investigating radicals and radical ions used as catalysts and reactive intermediates involved in novel photochemical reactions.

Each section of this thesis is further divided into chapters based on my published work. I selected topics that illustrate the development of my scientific career and to craft a compact narrative, starting from basic research and gradually moving to systems with increasing complexity. In discussing my published studies, I summarize the most important findings and specify their contribution and influence on the future development of the respective fields of knowledge. The publications are attached at the end of this thesis.

Photochemistry of Organic Molecules

Photochemistry and photophysics is based on light absorption, which induces electronic excitation of molecules. Due to their extreme versatility, organic molecules can be designed to absorb photons of specific energy. And while saturated hydrocarbons are inefficient absorbers, attaching functional groups known as *chromophores* increases their molar extinction coefficients in a specific wavelength region.

Chromophoric functional groups, most often based on double bonds (olefins and carbonyls), have a low energy gap between the highest occupied molecular orbital (HOMO) and the lowest unoccupied molecular orbital (LUMO). This energy gap determines the position of the absorption maximum of the entire molecule. Combining more chromophores through *conjugation* further decreases the energy gap between lowest and higher excited states and shifts the absorption to higher wavelengths from ultraviolet (UV) to visible and near-infrared (NIR) regions.

Most organic molecules are white powders and oils. However, since the 19th century, chemists have leveraged organic synthesis to produce highly coloured substances. These synthetic dyes soon replaced expensive natural dyes derived from various exotic sources, such as minerals, insects and roots. In 1856, while searching for a treatment for malaria, William Henry Perkin synthesized a substance with a brilliant purple hue, later named *Perkin's mauve* (Figure 1).[1] Soon after, synthetic dye production expanded, leading to the foundation of some of the oldest chemical companies, with BASF leading the way from the 1860s.

Over the years, some dyes were discovered by serendipity through condensation of different components into conjugated polycyclic chromophores. However, other dyes were designed by careful tuning their donor-acceptor properties, and hence the HOMO and LUMO energy. As a result, the famous BASF dye catalogue soon became filled with all desired hues and organic dye chemistry seemed to plateau.[2]

The industrial need for new pigments eventually declined, but the discovery of fluorescein by Alfold von Baeyer in 1871[3] changed the rules of the game. Fluorescence, a term that was coined by George Gabriel Stokes in 1852,[4] is the ability of dyes to emit light upon excitation. The difference between absorption and emission wavelength is called Stokes shift and is caused by molecular and solvent reorganization upon excitation.

Fluorescence quickly became a highly desired property, especially after development of fluorescence microscopy and imaging. Soon after Baeyer's discovery, rhodamines with red shifted absorption and emission spectra were introduced by Maurice Ceresole.[5] Together with cyanines, discovered in the 1970-1990s by a chemist and amateur photographer named Alan Waggoner,[6] they laid the foundations for the most successful fluorescent dyes used today (e.g., Cy5, Cy7, Texas red, Alexa Fluor®, and Atto dyes, among others).

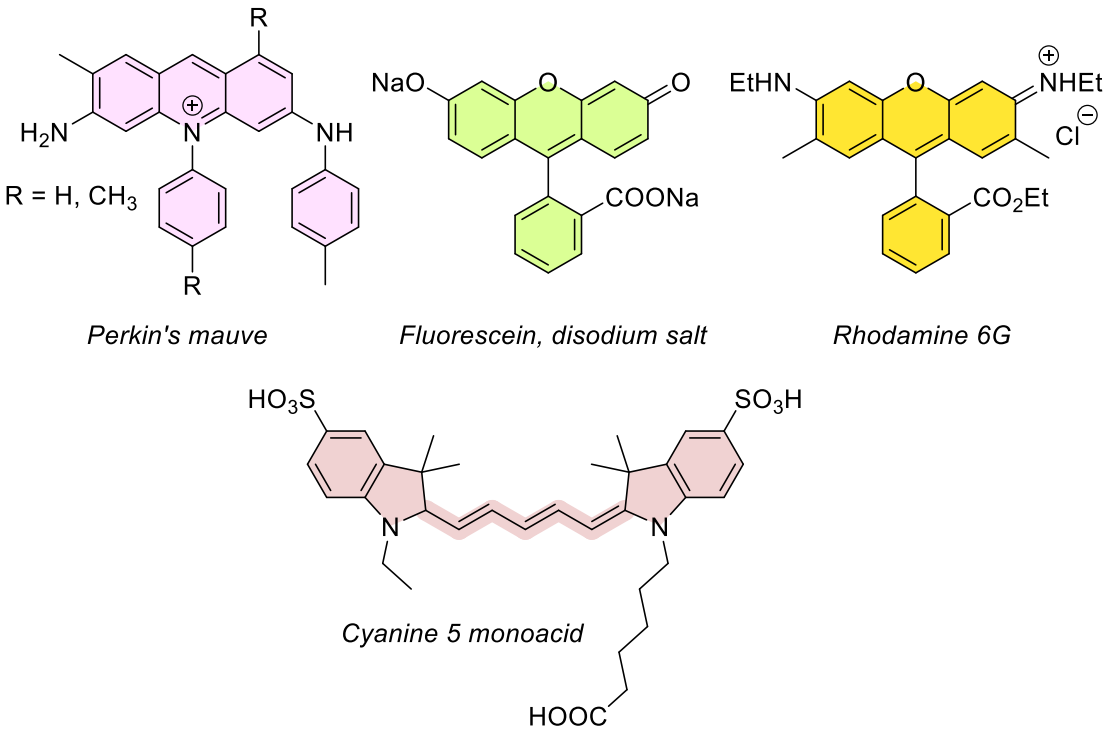

Figure 1: Perkin's mauve, Fluorescein, rhodamine and cyanine dye examples

1. Fundamental Principles: Excited-State Processes

Soon, it became obvious that not only light absorption but also the excited-state behaviour of organic molecules is crucial for any further use in photoactivation. A molecule in the electronically excited state can undergo a series of processes, which have been canonized by Aleksander Jabłoński in his famous diagram (Figure 2).[7,8] This diagram illustrates various electronic (thick horizontal lines) and vibrational (thin horizontal lines) states of a molecule with all radiative (straight arrows) and non-radiative (curly arrows) transitions. The Jabłoński diagram is used to describe excited-state dynamics and rates of photophysical and photochemical processes, such as fluorescence, internal conversion, vibrational relaxation, diabatic and non-diabatic photoreactions. A careful analysis of a Jabłoński diagram can therefore explain trends in excited-state behaviour, such as singlet-triplet compensation,[9] variation of fluorescence quantum yield as a function of molecular rigidity[10] and conical intersection control of photoreactivity.[11]

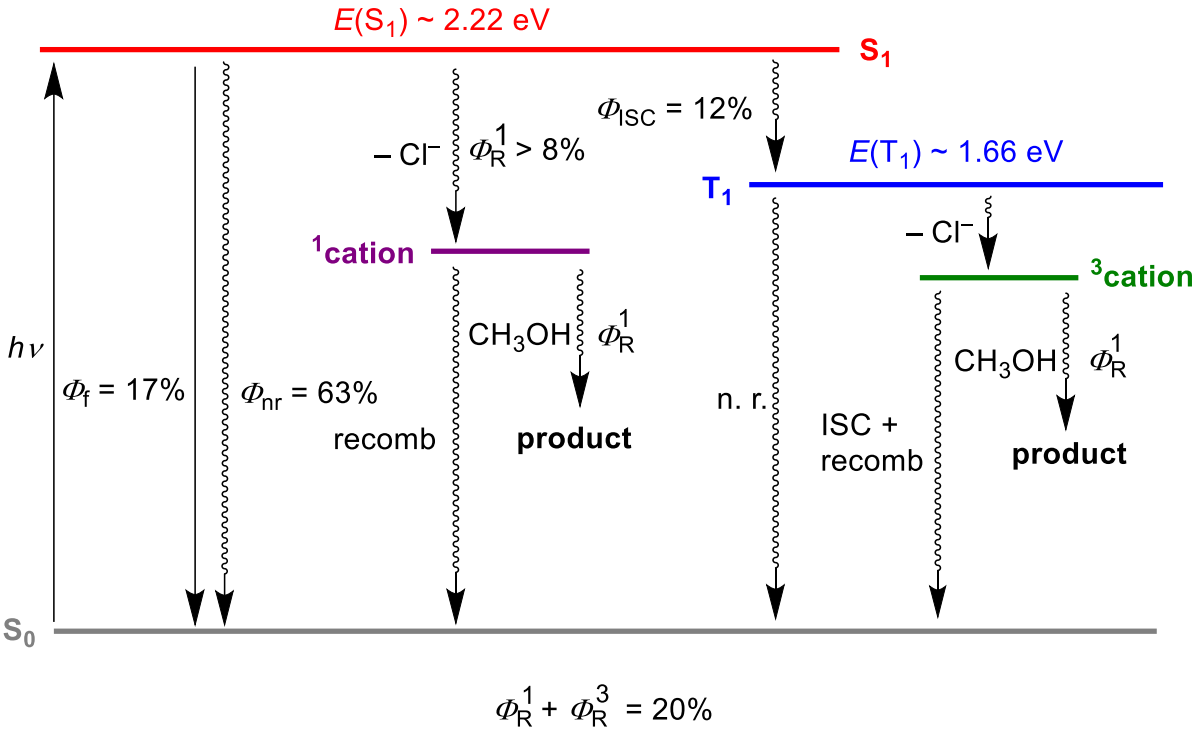

Figure 2: Example of Jabłoński diagram of BODIPY-based photoremovable protecting groups.[9] Quantum yields of Φ_f fluorescence, Φ_{nr} non-radiative decay, Φ_R reaction, Φ_{ISC} intersystem crossing.

1.1. Aromaticity: From Concepts to Overarching Theory

Introduction

The development of dyes has enabled us to study molecules with conjugated π-systems. And among all possible combinations, cyclic conjugated structures with a specific number of π-electrons were quickly identified as the best structural motifs. 6-π benzenoid structures, in particular, emerged as a central motif, ubiquitous in organic compounds.

Long debated, the structure of benzene was ultimately solved in 1865 by August Kekulé.[12] In his seminal paper, Kekulé proposed the correct structure of benzene, famously inspired by a dream of *ouroboros*, a mythical serpent eating its own tail. The exceptional stability of benzene was at first explained by *resonance* energy, caused by delocalization of π-electrons of its double bonds across the cyclic molecule. But other molecules with similar delocalization, such as 1,3-cyclobutadiene or 1,3,5,7-cyclooctatetraene (Figure 3), were destabilized and highly reactive. Erich Hückel explained this trend in 1931[13] when he proposed his famous rule according to which conjugated planar $4n+2$ π-electron systems are *aromatic* and stabilized, and $4n$ π-electron systems are *antiaromatic* and destabilized (n = 0,1,2…).

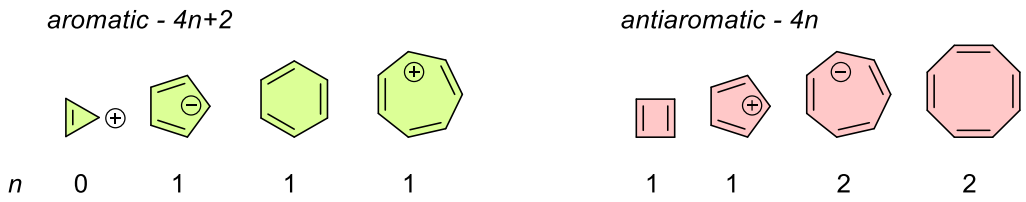

Figure 3: Examples of aromatic and antiaromatic hydrocarbon molecules and ions

Later on, the concept of aromaticity and antiaromaticity was expanded to heterocyclic molecules, non-benzenoid systems, spherical molecules, clusters of atoms and many other systems to which adding two extra electrons reverts their inherent stability/instability.[14,15] Most notably, in 1972, Colin Baird formulated yet another rule stating that the aromaticity of Hückel-aromatic systems reverts in the excited triplet state, meaning that $4n$ π-electron systems are excited-state *aromatic* and vice versa. This finding opened a completely new viewpoint for rationalizing the excited-state behaviour of organic molecules.

Benzene rearrangement[11]

Motivated by the reversal of chemical properties of aromatic molecules in the excited state, I studied the fundamental behaviour of the archetype aromatic molecule, benzene.[11] In collaboration with my postdoctoral supervisor, Professor Henrik Ottosson, at Uppsala University, Sweden, we focused on the photochemical rearrangement of benzene to bicyclo[3.1.0]hexene derivatives. This reaction was discovered in 1966 by Kaplan and colleagues (Figure 4a)[16] and was known only to illustrate that the excited-state chemistry of benzene was rich and unexpected, albeit for unknown reasons. Therefore, we aimed at explaining the reactivity and reaction mechanisms of this reaction and at optimizing the process, thereby making it synthetically useful.

In this reaction, three chiral centres were installed into the originally planar benzene molecule. Primary and secondary photochemical and thermal processes equilibrated the mixture of more than 4000 formed products into a handful of isomers. Upon optimization, the most photochemically inert and thermally stable isomer, formed with chemical yield of up to 75%, was separated from the reaction mixture and enzymatically derivatized to give access to a single enantiomer with potential use in medicinal chemistry.

In our study, we tested two major mechanistic hypotheses involving excited-state antiaromaticity alleviation of benzene in its S_1 state (Figure 4b). While protonation directly from the S_1 state to bicyclo[3.1.0]hexenium cation was too slow to compete with other processes, S_1 benzene rearrangement to benzvalene, followed by protonation and nucleophilic substitution, was the operative mechanism. Moreover, we tamed the destabilization of excited-state benzene, thereby synthesizing complex three-dimensional molecular scaffolds that can be used as pharmacophore linkers in drug design. This research reignited chemists' interest in early photochemical processes because they could be now rationalized, understood and optimized through the theory of excited-state aromaticity.

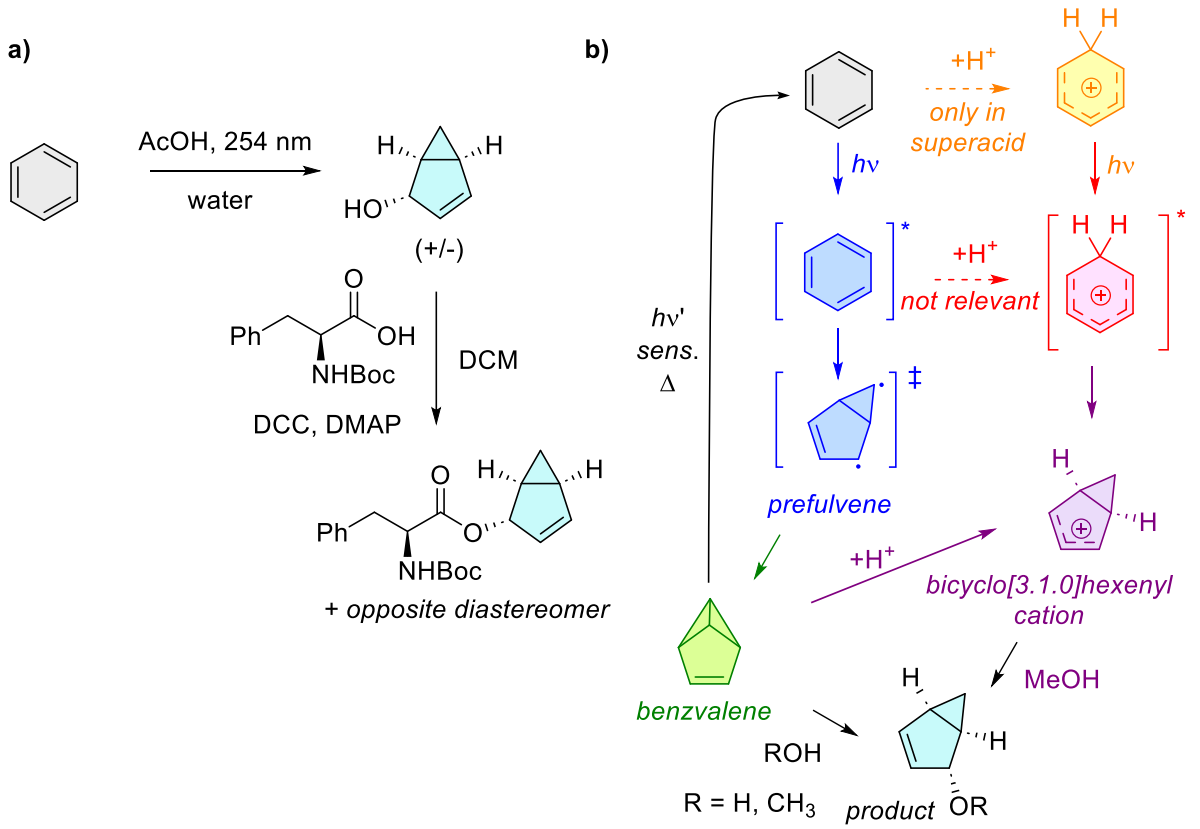

Figure 4: a) photochemical rearrangement of benzene to bicyclo[3.1.0]hexene derivatives and its further derivatization to diastereomeric esters b) mechanism of benzene rearrangement. Orange pathway is relevant only in superacidic media, red pathway occurs but does not compete with benzene rearrangement to benzvalene (blue pathway). Benzvalene in acidic media is protonated to bicyclo[3.1.0]hexenyl cation (violet pathway) or reacts directly with solvent to form the bicyclic product.

Azulene photophysics[17]

Aromatic and antiaromatic rules have been used to describe the behaviour of the most abundant class of aromatic molecules, benzenoid aromates. While theoretically studying various aromatic molecules, we followed how minor structural alterations in benzenoid naphthalene resulted in its conversion into the isoelectronic isomer, non-benzenoid *azulene*. Azulene is a molecule with unique and unexpected properties, which cannot be explained by the state-of-the-art theory. In fact, this molecule has raised many questions since its discovery by Septimus Piesse in 1863[18] and its structural elucidation by Lavoslav Ružička in 1931.[19] While naphthalene is white, azulene has an intense blue hue and exists as a natural dye in mushrooms, chamomile and many other plants (Figure 5a).[20] Azulene's blue hue was eventually explained by J. Michl in the 1970s,[21] but its emission behaviour remained a puzzle long after. Unlike all other simple aromatic hydrocarbons, azulene does not emit from its first excited singlet state, S_1, but from its higher excited S_2 state. Therefore, azulene thus does not obey the Kasha's rule according to which '*the emitting level of a given multiplicity is the lowest excited level of that multiplicity*'.[22]

To explain this exotic behaviour of azulene, we computed azulene's electronic structure of various electronic states of singlet (S_0, S_1, S_2), triplet (T_1) and quintet (Qu_1) multiplicity.[17] We used the perturbational molecular orbital theory (PMO), developed by Baird for describing excited-state (anti)aromaticity, for fused bicyclic systems, and proposed a model explaining the photophysical properties of azulene according to the excited-state (anti)aromaticity of its different electronic states. Based on various aromaticity indices, our model (Figure 5b) showed the (i) contrasting (anti)aromaticity of the first and second excited singlet states of azulene and an (ii) easily accessible antiaromaticity relief pathway through a conical intersection between antiaromatic S_1 and aromatic S_0 state. Measured by ultrafast transient pump probe spectroscopy, excited-state dynamics confirmed the model and showed a distinct lifetime difference between S_1 and S_2 states (ps vs ns).

This study not only broadens the PMO theory to non-benzenoid aromates and rationalizes the design of anti-Kasha fluorophores but also demonstrates that azulene has no transannular delocalization, a misconception that can be found in many organic chemistry textbooks when explaining the high dipole moment of azulene (Figure 5c).

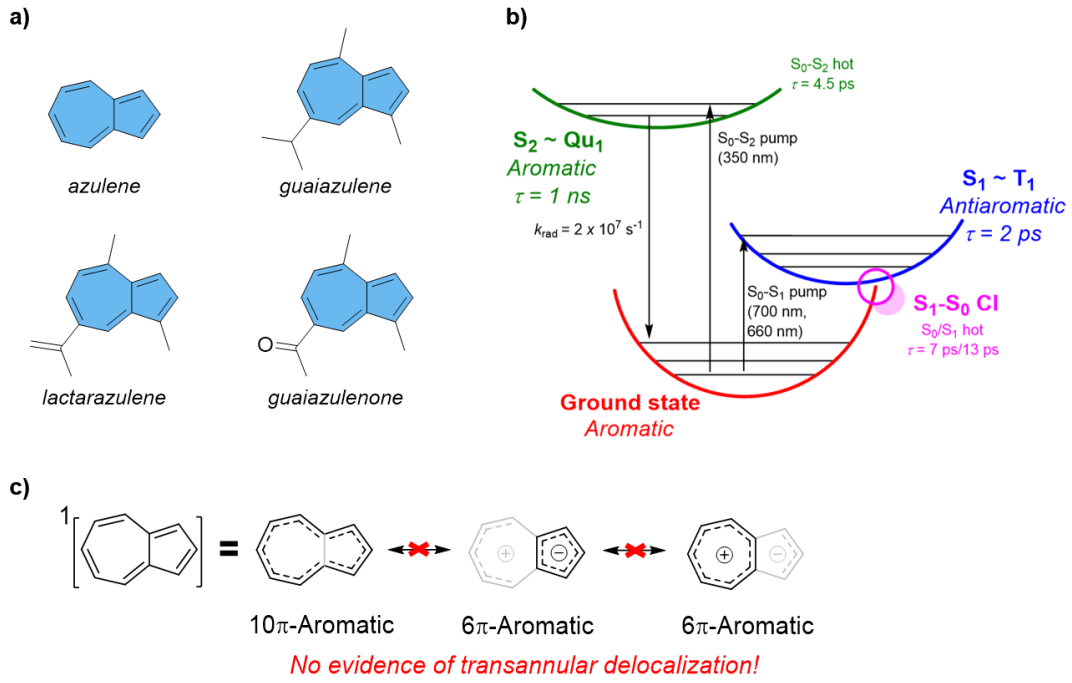

Figure 5: a) azulene and its derivatives found in nature, b) Jabłoński diagram demonstrating its anti-Kasha behaviour, c) azulene's resonance structures found in organic textbooks.

Photodegradation of pharmaceuticals[23]

In our search for systems whose behaviour can be rationalized by excited-state (anti)aromaticity, we teamed up with AstraZeneca in Göteborg, Sweden. This company is deeply interested in understanding the photodegradation of pharmaceuticals. As most small-molecule drugs are heteroaromatic compounds, irradiation prompts their antiaromatic excited states, seeking a path to alleviate this antiaromaticity. Focusing on the amiloride family, which

is plagued by photodegradation, with associated toxicity,[23] we subjected an amiloride model to efficient photosubstitution in an alcoholic solvent, avoiding photodehalogenation (Figure 6a). In doing so, we found that amiloride undergoes a unique photoionization mechanism, forming a radical cation that reacts with the protic solvent.

This work demonstrates that antiaromaticity alleviation, which leads to the ejection of electrons into the solvent, is a general pathway for electron-rich aromatic heterocycles with large HOMO-LUMO orbital splitting. Ground-state antiaromatic derivatives have low-lying LUMO, which does not facilitate the photoionization (Figure 6b). By contrast, aromatic analogues have LUMO closer to the ionized state energy level and, hence, higher propensity to electron ejection from the excited state.

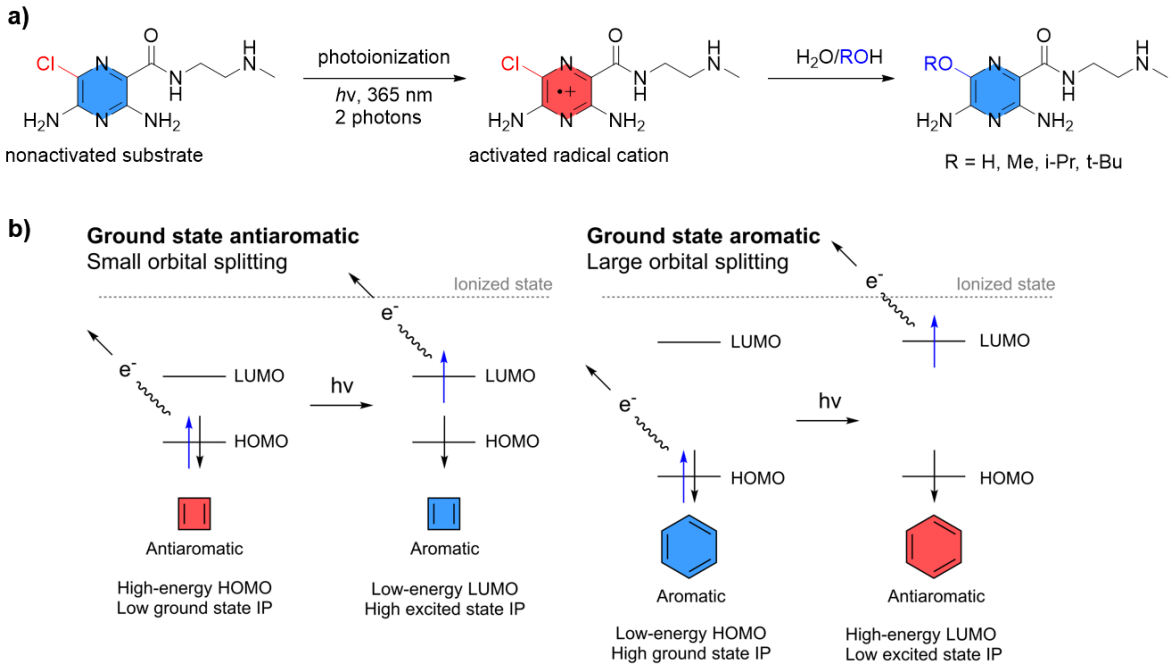

Figure 6: a) photodegradation of amiloride model caused by excited state antiaromaticity, b) relationship of (anti)aromaticity and ionization potential of organic molecules.

Excited state (anti)aromaticity-driven photochemistry[24]

We later realized that excited-state antiaromaticity relief and excited-state aromaticity gain are the driving forces of many different types of photoreactivity. In our review paper,[24] we summarized various effects of excited-state (anti)aromaticity (ES(A)A) on the excited-state behaviour of various molecules. Specifically, we discuss the ES(A)A effects on the excited-state energy surfaces, controlling molecular emission, Stokes shift, puckering, and ring-opening reactions. In addition, we discussed that excited-state aromaticity accounts for the lack of photoreactivity of ground-state antiaromatic molecules (1,3-cyclobutadiene, 1,3,5,7-cyclooctatetraene, fluorenyl cation, dibenzo oxepin and suberene derivatives) and for the rich photochemistry of ground-state aromatic molecules (rearrangement of benzene derivatives, photoacidity of phenols, ESIPT, dearomatization processes, electron transfer, and photocleavage). This review showed the universality of ES(A)A rules on the behaviour of

ground- and excited-state planar conjugated organic molecules and, as such, laid the foundations for a general theory explaining the inverse trends of ground- and excited-state chemistry.

1.2. Triplet Chromophores: Heavy Atom Substitution

Introduction

While most of the early research on chromophores focused on their absorption and fluorescence, in 1873, Hermann Wilhelm Vogel realized the untapped potential of excited molecules. Vogel studied early photographic materials that were most sensitive to UV and blue light, which made blue objects lighter than red objects in photographs.[25,26] He discovered that adding some dyes, termed *photosensitizers*, enhanced the spectral range of these emulsions. These dyes absorb visible light and transfer their energy to silver bromide, producing Ag^0. These findings fostered the commercial development of black-and-white film that responded to light across the visible spectrum.

Triplet excited states of dyes were later identified as key players in photochemical reactions.[27] Because most organic molecules do not undergo efficient intersystem crossing, triplet-triplet sensitization was introduced in the 1960s as an efficient method for reaching triplet states inaccessible by direct excitation.[28]

Excited triplets of organic molecules have a long lifetime (μs to ms) and, in line with the multiplicity selection rules, efficiently interact only with other molecules in the triplet state. The most abundant molecule with a triplet ground state is dioxygen ($^3O_2$), which is efficiently sensitized by excited triplet chromophores. The product of this sensitization, *singlet oxygen* ($^1O_2$) is a highly reactive species that oxidizes organic substrates and other molecules in its proximity. Considering their relatively high triplet energy, organic fluorophores with a high intersystem crossing quantum yield were introduced as efficient photosensitizers for singlet oxygen production. Triplet sensitization led to the development of *photodynamic therapy*, a technique whereby a photosensitizer is administered in body and accumulates in malignant tissue. This tissue is irradiated, usually with red-NIR light, which penetrates deep into tissues. In tissues, the photosensitizer produces singlet oxygen, which oxidatively destroys nearby cells. Porphyrins were the first photodynamic dyes,[29,30] and the scope of suitable photosensitizers has been later extended to phthalocyanines and other triplet chromophores.[31]

BODIPY dyes with heavy-atom substitution[32,33]

Triplet photosensitizers were first identified for their ability to produce singlet oxygen. Subsequently, with the development of transient absorption spectroscopy and other time-resolved spectroscopic techniques, efficient intersystem crossing and long triplet lifetime were identified as the key parameters of a successful triplet photosensitizer. The most efficient strategy of triplet photosensitizer design is heavy-atom substitution of their π-system. This *heavy atom effect* enhances spin-orbit coupling and enables the multiplicity change between singlet and triplet states.

The most common heavy-atom used to enhance the intersystem crossing rate is iodine. Its effect on fluororophore photophysical properties is shown by marked changes in the fluorescence and triplet quantum yield of BODIPY chromophores. While the parent compound has 92% fluorescence quantum yield and negligible triplet, its iodinated analogue has a significantly suppressed fluorescence (Φ_{fl} = 5%) and 54% intersystem crossing quantum yield (Figure 7a).[32] Attaching iodine atoms onto fluorophores may seem an excellent method for inducing efficient triplet formation, but their photostability is low due to the photoinduced cleavage of the weak C – I bond (Figure 7b). This fact disqualifies most iodinated fluorophores as photosensitizers. For this reason, in collaboration with Prof. Petr Klán, Masaryk University, Brno, we attached various heavy chalcogen atoms onto BODIPY to prepare more photostable photosensitizers (Figure 7c).[32,33]

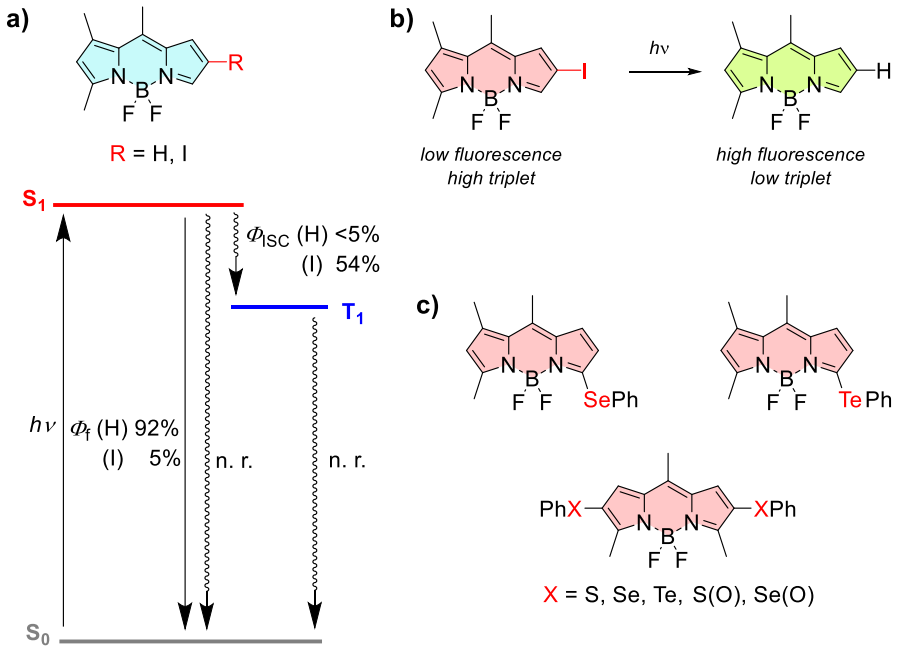

Figure 7: a) excited state characteristics of BODIPY and its iodinated analogue, b) photodehalogenation reactivity, b) chalcogen-substituted BODIPY photosensitizers

For this purpose, we first attached selenium and tellurium-containing substituents onto the position 1 of the BODIPY scaffold. This substitution was easy due to the simple addition-elimination substitution of halogen atoms in α-position of pyrroles. Attaching just one selenium or tellurium atom enhanced the triplet yield to 74%, almost as high as in the case of iodo-substituted derivative. The compounds, however, did not exhibit any photodegradation and therefore could serve as perspective photosensitizers.

Our more rigorous study on symmetric, di-chalcogenated BODIPY derivatives revealed surprising trends.[33] Attaching two heavy atoms onto positions 2 and 6 should further increase intersystem crossing quantum yields. But attaching a chalcogen onto position 2 was less efficient than onto position 1, likely due to the symmetry and nodal planes of active orbitals involved in the intersystem crossing. In addition, symmetrically attaching two chalcogens into positions 2 and 6 formed a twisted intramolecular charge transfer state, which supressed both fluorescence and intersystem crossing. These studies show that using heavy chalcogens as

heavy atoms instead of iodine leads to photostable photosensitizers, but the low oxidation potential of tellurium, in particular, leads to photoinduced charge transfer processes between the chalcogen moiety and the excited BODIPY fluorophore.

Chalcogenated BODIPYs as sensors[34]

We used this property of chalcogenated BODIPYs to efficiently produce an intramolecular charge transfer (ICT) state to design fluorogenic sensors for oxidative stress. The ICT state of chalcogen-substituted BODIPY has weak, red-shifted fluorescence, whose maximum depends on the solvent polarity. Oxidation of the chalcogen (S, Se) to the corresponding chalcogenoxide restores the strong locally excited emission with small Stokes shifts, typical of unsubstituted BODIPYs. The oxidation product can be further reverted back to the initial state by reduction agents. The oxidation state of the dye may therefore reflect the redox potential of the surroundings and manifest this change through a distinct change in fluorescence.

With this idea in mind, we designed a series of mono- and di-substituted BODIPYs with sulfur or selenium moieties (SMe, SPh and SePh) in positions 2 and 6 (Figure 8a). Our initial screening with various oxidants and reductants revealed high chemoselectivity to perchlorates (oxidation) and hydrogen sulfide (reduction). Selenium derivatives had a redox potential closer to that of biologically relevant targets, but the sulfur derivatives were more chemically stable. As in our previous study,[33] symmetric, disubstituted derivatives formed an efficient ICT state, while non-symmetric analogues (SPh, SOPh) had efficient intersystem crossing.

Installing polar sulfonate groups improved the aqueous solubility of BODIPY probes while retaining their sensing properties, thus enabling us to use these fluorescence probes to monitor the enzymatic activity of enantioselective methionine sulfoxide reductase MsrA (Figure 8b). This study shows that the photophysical properties of BODIPY can be modulated by substitution with chalcogen atoms, leading to triplet or ICT states. Due to its small size, BODIPY is an excellent fluorescence sensor for monitoring enzymatic activity because it fits into the active site of many enzymes. Moreover, sulfoxides and selenoxides are chiral, enabling enantioselective sensing.

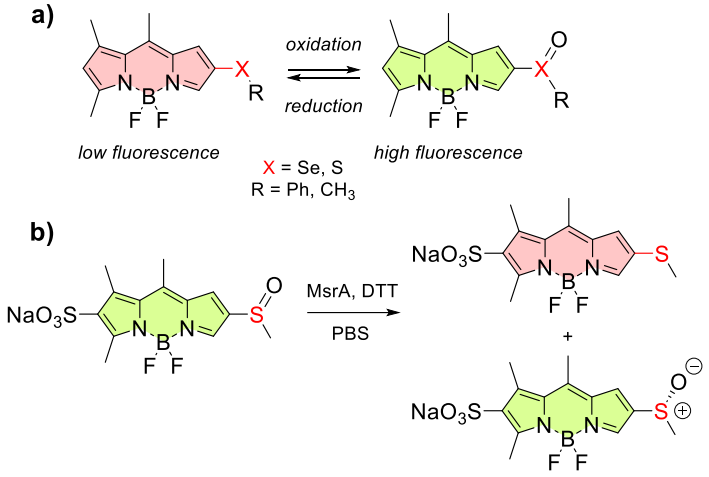

Figure 8: a) chalcogen-substituted BODIPY sensors, b) fluorescence sensing of MsrA activity (DTT = dithiothreitol)

2. Photocontrolled Functional Molecules

After structure, molecular *function* became one of the most important targets of molecular design in contemporary chemistry. The research of functional molecules gradually moves from *permanent* function to *programmable* and *controlled* function that can be activated, switched or modulated by external stimulus. As an excellent external stimulus, light can be precisely controlled in space and time and is by nature completely traceless. The development of precise and high-intense light sources, such as LEDs and lasers, has fostered the development of light-triggered functional molecules with a specific function. Therefore, the complex environment of tissues and living organisms can be remotely controlled by light, inducing various effects (signalling, therapeutic effect, adjustment of cellular milieu, regulation of gene expression, construction or destruction of various structures, among other effects).[35–38] Photocontrolled functional molecules can be categorized by their function into three categories, namely molecules that cleave a chemical bond – *photocages* –, processes that form a chemical bond – *photoclick* reactions –, and derivatives that reversibly isomerize upon absorption of light – *photoswitches*.

2.1. Photocages

Photocages (photoremovable protecting groups or photocleavable compounds) are molecules that can cleave a chemical bond upon irradiation with light.[39] Photocages were originally developed in the 1960s to temporarily protect reactive functional groups in organic synthesis.[40–43] In the following decade, Engels, Schlaeger and Kaplan synthesized protected cyclic adenosine monophosphate (cAMP) and ATP, the first examples of biologically active caged molecules.[44,45] Since then, photocaging has been gradually used in a wide range of applications aimed at releasing chemicals, such as bioagents, neurotransmitters, cell-signalling molecules, acids, bases, ions, oxidants, insecticides, pheromones, and fragrances, among others.[10,39] But until 2015, all photocages showed suboptimal absorption and quantum yields and limited biocompatibility. Only the latest advances in the state of the art have enabled us to overcome these limitations, particularly in the development of UV photocages and efforts to activate photocages with visible light.

UV photocages[46,47]

In 2007, I started my scientific career in Professor Klán's research group at Masaryk University, Brno. Working with UV-activatable photocages, we studied the benzoin photocage, the only photocage where the leaving group was attached at an enantiotopic position, making the whole construct chiral (Figure 9a). Although the presence of a stereogenic centre in a photocage had long been considered a disadvantage, we utilized the chirality of benzoin in a *photoremovable chiral auxiliary*, a group attached to a prochiral substrate to induce a diastereoselective transformation and to be photochemically removed, thereby releasing a

chiral product. Using this approach, we synthesized enantiopure benzoin-protected acrylates that underwent Diels-Alder [4+2]-cycloaddition with cyclopentadiene to norbornene esters in a diastereoselective manner. Upon photochemical deprotection of the photoremovable chiral auxiliary, chiral norbornene carboxylic acids were produced in a high enantiomeric excess (of up to 96% ee). This study showed that chirality, such a unique property of benzoin photocages, widely regarded as a 'bug' in the system by the scientific community, could be leveraged into a feature when approached in the right way and thus so could others.

Another 'bug' of UV photocaging was the limited scope of leaving groups that can be released by irradiation. Only anions of strong acids, such as sulfonates and halides (iodide, bromide, and chloride) were released with high quantum yields. Anions of weak acids, such as carboxylates, alcohols, phenols, and thiols, required long irradiation times due to their low quantum yields of photorelease. In addition, the photochemistry of caged weak acids was usually complex, leading to mixtures of photoproducts.[38] Therefore, caging weak acids required using reliable photocages with *high expulsion power*, i.e., with the ability to photocleave strong bonds between the photocage and the leaving group.

Early photocages, such as benzoin, *ortho*-nitrobenzyl or phenacyl groups, had low expulsion power and could only be used for strong acids. However, Givens et al. eventually developed a *para*-hydroxyphenacyl photocage with a significantly different mechanism and with a much stronger expulsion power than phenacyls.[48] While phenacyls cleaved the leaving group through a photoinduced radical pathway, *para*- and *ortho*-hydroxy[49] derivatives photocleaved the leaving group through a *photo-Favorskii* rearrangement to hydroxyphenyl acetic acid (Figure 9b).

Motivated by the reliable and clean photochemistry of *para*-hydroxyphenacyl photocages, in collaboration with Professors Klán and Givens, we synthesized *para*-hydroxyphenacyl fluoride (Figure 9c).[47] Fluoride was quantitatively released, with a high quantum yield of 83%. Moreover, the photorelease varied with the pH, markedly decreasing in efficiency under basic conditions (pH = 10). This relationship reflects the large energy difference between the neutral triplet of *para*-hydroxyphenacyl moiety and its corresponding triplet anion.[50] Only the neutral form of the excited triplet state had enough expulsion power to release the fluoride from its structure.

Next, we demonstrated that fluoride release could be spatially resolved for surface etching. For this purpose, we applied a homogeneous layer of caged fluoride on the surface of silicon or mica and monitored the etching by photoreleased fluoride by atomic force microscopy, thus significantly advanced fluoride photoetching technology. Unlike state-of-the-art methods, which require a multistep procedure using photomasks, we can now directly etch surfaces in a single step by focused UV light using this approach.

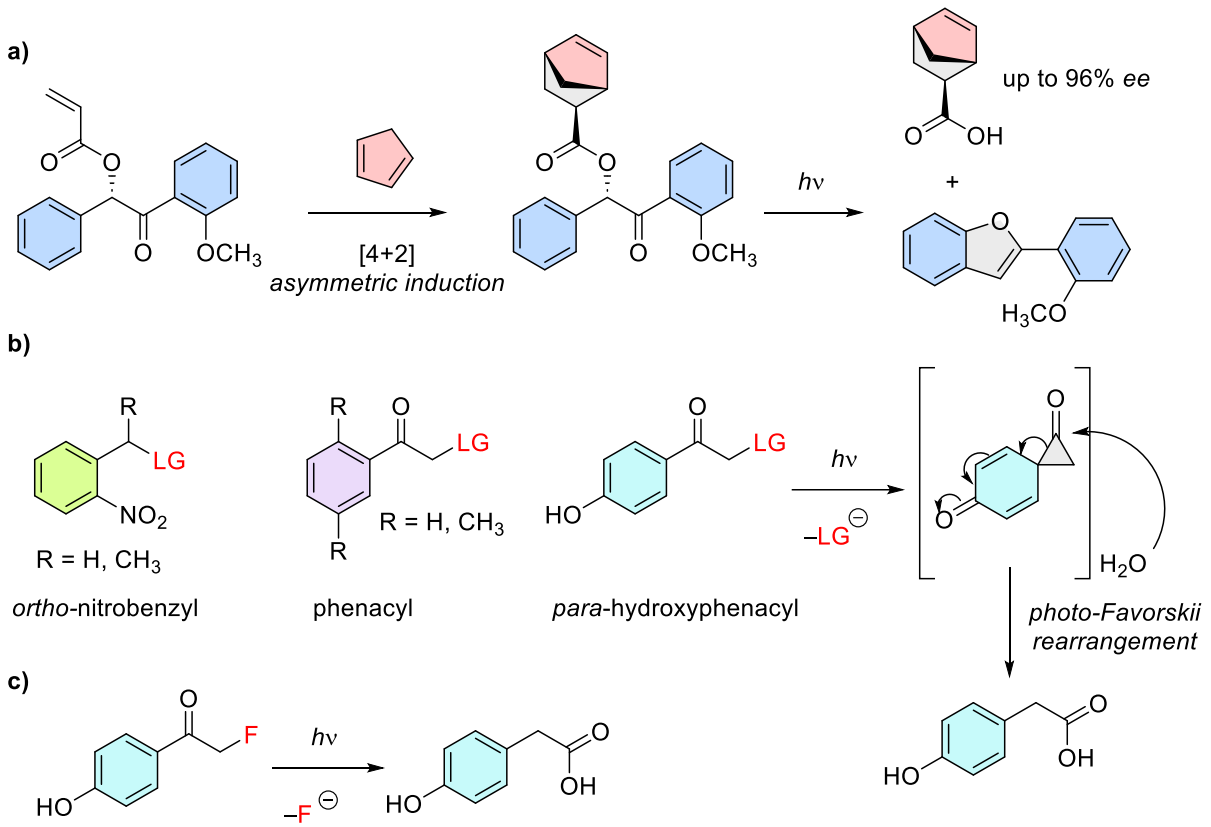

Figure 9: a) benzoin-based photoremovable chiral auxiliary, b) common UV-photocages, mechanism of 4-hydroxyphenacyl photorelease *via photo*-Favorskii rearrangement, c) photochemical release of fluoride from 4-hydroxyphenacyl fluoride

Towards visible light activation[51,52]

In 2010, when I entered this field of research, all known photocages were activated by UV light. The common belief was that visible light photons did not have enough energy to cleave a covalent chemical bond. Nevertheless, we wondered whether shifting the absorption of UV photocages to the visible range would release the leaving group upon irradiation.

We tackled this challenge by installing *push-pull* and *π-extending* substituents on UV-absorbing 3-diethylaminobenzyl photocages developed by Zimmerman[53] to bring HOMO and LUMO levels closer and hence shift the absorption into the visible region (Figure 10a,b).[51] In collaboration with Professor Alexander Heckel from Goethe University in Frankfurt am Main, we synthesized and characterized a series of 3-diethylaminobenzyl derivatives as cages for glutamic acid. Attaching strong electron-donating and -withdrawing groups in a 1,4-arrangement induced an absorption maximum at the blue edge of the visible region by creating a new charge-transfer absorption band, but excitation into this band did not lead to the release of glutamic acid. At this point, we realized that efficient photocleavage required redistributing the electron density in the excited state to induce significant *antibonding character* of the 'photocage-leaving group' bond. By contrast, in push-pull systems, excitation populated the charge-transfer state, where the electron density was pushed from the electron-donating to the electron-accepting group, with no effect on the 'photocage-leaving group' bond.

Attaching substituted phenyls did not enhance visible light absorption as the new π-system was perpendicular to the 3-diethylaminobenzyl system and hence failed to extend π-conjugation. However, locking the new phenyl with a methylene bridge, forming fluorenyl derivatives, improved the UV absorption properties and increased the photorelease quantum yields (from ~4 up to 42%) thanks to the excited-state aromaticity of the fluorenyl cation, formed by photocleavage (Figure 10c). This study shows that the absorption of a photocage in the visible region alone may not suffice for visible-light induced photorelease of the leaving group, but other properties, especially the antibonding character of the 'photocage-leaving group' bond, play the key role.

The findings described above informed us that more sophisticated design strategies must be used to induce visible light photocleavage. Accordingly, in collaboration with one of the greatest minds in photochemistry of the last century, Professor Joggi Wirz, from the University of Basel, Switzerland, we approached the design of visible light photocages based on *extended Hückel theory*.[54] Considering the position of nodal planes in HOMO and LUMO, this approach reliably predicted electron density redistribution upon excitation. In addition, we found that many common fluorescent dyes (coumarines, xanthenes, rhodamines, cyanines, and BODIPYs) had similar nodal plane symmetry, with a nodal plane in HOMO and large orbital coefficient in LUMO for the *meso*-position (Figure 10d-f). Attaching a methyl, substituted with a leaving group, to this position increased antibonding character of the 'photocage-leaving group' bond in the excited state, which facilitated the photosolvolysis (*via* photo-S_NAr pathway).

Based on this theory, we designed a fluorescein analog with *meso*-methyl substitution to release leaving groups upon green light irradiation.[52] While the design was straightforward and involved a xanthene moiety commonly used as a chromophore, we discovered that attaching a non-aryl substituent to the *meso*-methyl position was challenging. After years of attempts, we synthesized the target fluorescein derivative as a non-covalent complex with 2,3-dichloro-5,6-dicyano-1,4-benzoquinone (DDQ), which was used in the last synthesis step and inseparable from the final compound. Irradiation with green light released the leaving group, making this molecule the *first visible light activatable photocage*. The photoproduct was identified as a xanthene carboxylic acid (*vide infra*) formed by oxidation of the photosolvolytic alcoholic product.

This study was a breakthrough in photocage development. It introduced a new paradigm according to which photon energy does not need to be higher than the strength of the bond between the photocage and the leaving group. The increase in its antibonding character in the excited state alone weakens the 'photocage-leaving group bond' and facilitates the solvolysis process. While groundbreaking, the fluorescein photocages were nevertheless only rarely used for photocaging due to their limited synthetic availability.

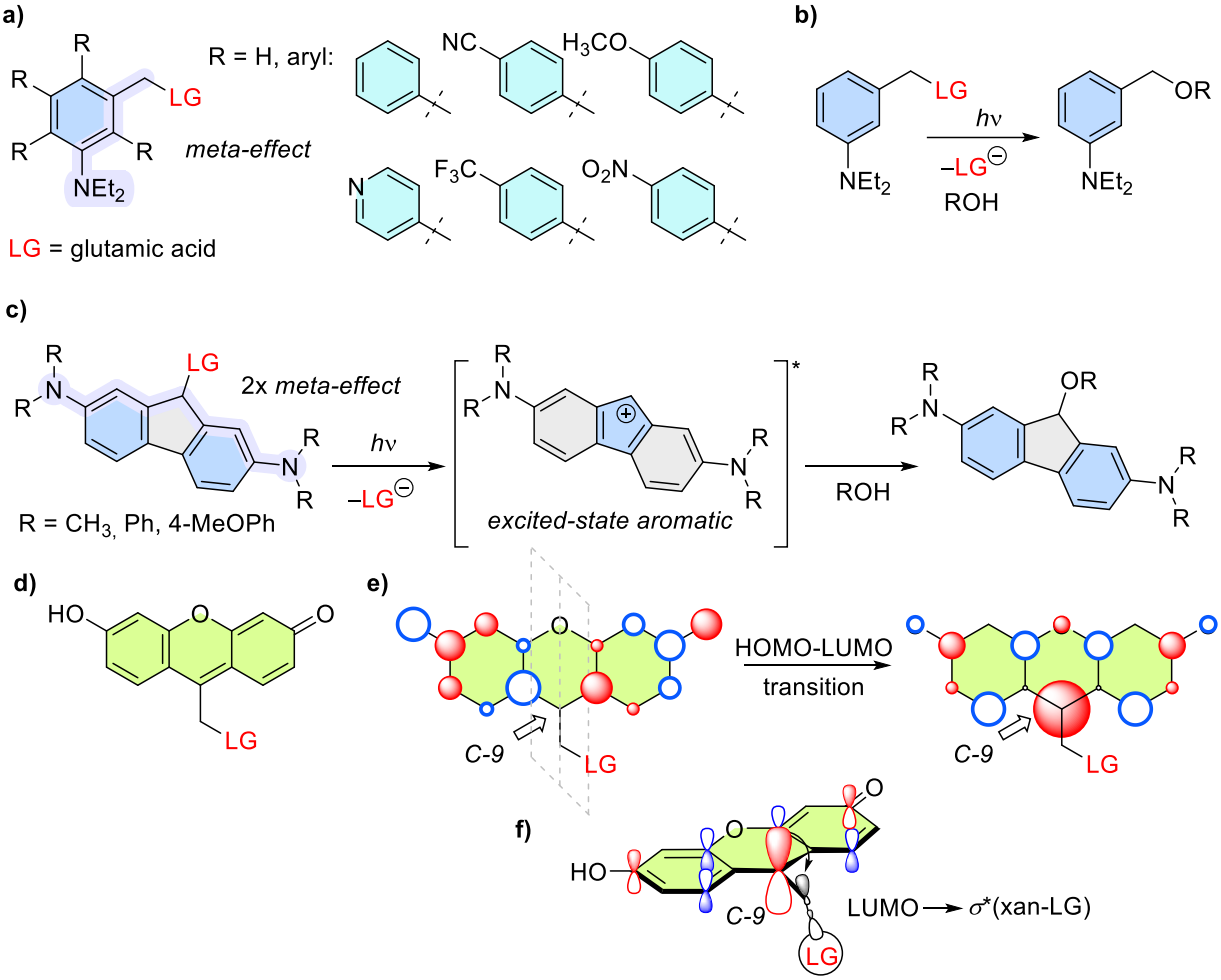

Figure 10: a) 3-diethylaminobenzyl *meta*-effect-based photocages, b) their uncaging *via* photosolvolysis, c) fluorenyl photocage forming excited state aromatic carbocation, d) structure of the first visible-light absorbing xanthene-based photocage, e) extended Hückel-based molecular orbital diagram of HOMO (left) and LUMO (right) showing a buildup of electron density in the C-9 (*meso*) position, f) hyperconjugation donation of electron density in LUMO to the antibonding orbital of xanthene-LG bond.

From serendipity to a new paradigm[9,10,55,56]

Because xanthene-based photocages were synthetically challenging, we synthesized their pyronin analogs (Figure 11a). The synthetic intermediate, 1,3-dithianyl derivative, planned as a carbaldehyde precursor for further reduction to the desired synthetic target, photochemically decomposed to a xanthenone upon irradiation with yellow light.[57] This finding was even more controversial than the photorelease from fluorescein-based photocages. How could a yellow photon (590 nm, 2.1 eV, 48 kcal/mol) cleave a C–C covalent bond (~80 – 100 kcal/mol)?![58] Challenged by this finding, we analyzed in detail the photoreaction mechanism, in collaboration with Professor Jana Roithová at Nijmegen University, the Netherlands. The results showed that the transformation from dithianyl derivative to xanthenone is a multistep process, involving dithiante photodeprotection to carbaldehyde followed by a photoinduced Dakin rearrangement to enol ether and hydrolysis to the final product.[55] The key finding of

this study was that a multistep process involving the absorption of several visible light photons may cleave a strong bond even when a single visible photon lacks energy to break such a bond. Such a multistep multiphoton process plays a key role in photochemical bleaching of common fluorescent dyes.[59]

As mentioned above, the fluorescein-based photocage revolutionized photochemistry, prompting chemists to develop visible light-activatable photocages, including us. By January 2015, we were finalizing a manuscript on *meso*-methyl *BODIPY photocages* (Figure 11b) designed based on our extended-Hückel theory model of weakening chemical bonds by increasing the antibonding character of the 'photocage-leaving group' bond in the excited state (*vide supra*). However, a week before submitting the manuscript, we were scooped by the research groups of Professor Art Winter, at Iowa State University, USA, and of Dr. Roy Weinstain, at Tel-Aviv University, Israel, who introduced these derivatives as photocages in two studies published in *J. Am. Chem. Soc.*[60] and *Chem. Commun.*[61], respectively. In both research groups, the same photocage structure had been designed using completely different approaches. Art Winter's group used simplified molecular orbital theory, whereas Roy Weinstain's group derived the reactivity from coumarinyl photocages.

Unable to publish our results, we asked these groups to collaborate with us on a larger project aimed at explaining the mechanism of photorelease and optimizing photochemical quantum yields. The first generation of BODIPY photocages absorbed green light and had extremely low uncaging photorelease quantum yields (~10^{-4}). As such, they were impractical for releasing large amounts of caged substrates.

Through our mechanistic analysis, we gained detailed insights into the mechanism of photorelease, which enabled us to cooperatively enhance the photorelease efficiency of BODIPY photocages. By optimizing the structure at almost all positions of the parent BODIPY, we tuned the photocage expulsion power and multiplicity of the operative excited state, thereby increasing the photorelease quantum yield by four orders of magnitude to its physical limit (up to 95%).[9] As a result, these second-generation BODIPY photocages became the most efficient visible light absorbing photocages. This study epitomizes fine-tuning structure-activity relationships as a strategy for optimizing photorelease quantum yield, ultimately showing that visible light can be used for biological purposes.[10]

The next challenge in photocage development was to further shift the absorption to the red-to-near-infrared region. This wavelength region approximately overlaps with the *tissue-transparent* or *phototherapeutic window* between 650 and 900 nm because mammalian tissues are highly optically dense, containing many chromophores, such as hemoglobin, melanin, and bilirubin. In other words, this is the region where mammalian tissues are most transparent to light and is thus used for deep-tissue irradiation.[62,63]

Deep tissue photorelease of biologically active molecules, such as therapeutics or signaling molecules, is an emerging area of research with potential applications in biology, pharmacology and medicine. These applications range from spatiotemporally controlled targeted drug delivery for minimally invasive therapy with reduced side effects to disease diagnosis and personalized medicine. We therefore strived to develop red-NIR absorbing photocages.

We based our design on green light-absorbing BODIPY photocages described above. Assuming that visible light photons had enough energy to facilitate photocleavage, we

synthesized π-extended, distyrylated BODIPY photocages (Figure 11c) absorbing in the region between 650 and 700 nm.[56] Yet, despite using design principles learned in the structure-reactivity optimization of green-light-absorbing BODIPYs, we found that the photorelease quantum yields were low (~10^{-5}) due to the energy gap law.[64] According to the energy-gap law, the energy of the lowest excited states of red-absorbing BODIPYs is so low that non-radiative processes compete with photorelease, reducing the overall photorelease efficiency.

These BODIPY photocages had, nevertheless, high extinction coefficients and hence reasonable uncaging cross-sections, so we used them to release signaling molecules requiring minimal amounts of the released leaving group for the desired cellular response. By attaching sulfonate solubilizing groups and oleic acid as a model signaling molecule, we converted these photocages into amphiphilic molecules, which caused their accumulation in cellular membranes. The more charged, disulfonated analog did not penetrate into cells and selectively stained the plasmatic cellular membrane, whereas the least polar, mono-sulfonated photocage stained the internal membranes of organelles. With precise laser irradiation, we were able to show that oleic acid was selectively released in different cellular compartments. This compartmentalized release led to differentiated responses of Ca^{2+} oscillations, a model signaling pathway used to monitor oleic acid release.[56] This study fostered the first biological application of red-absorbing photocages, inducing a macroscopic change in cellular metabolism upon the photorelease of signaling molecules.

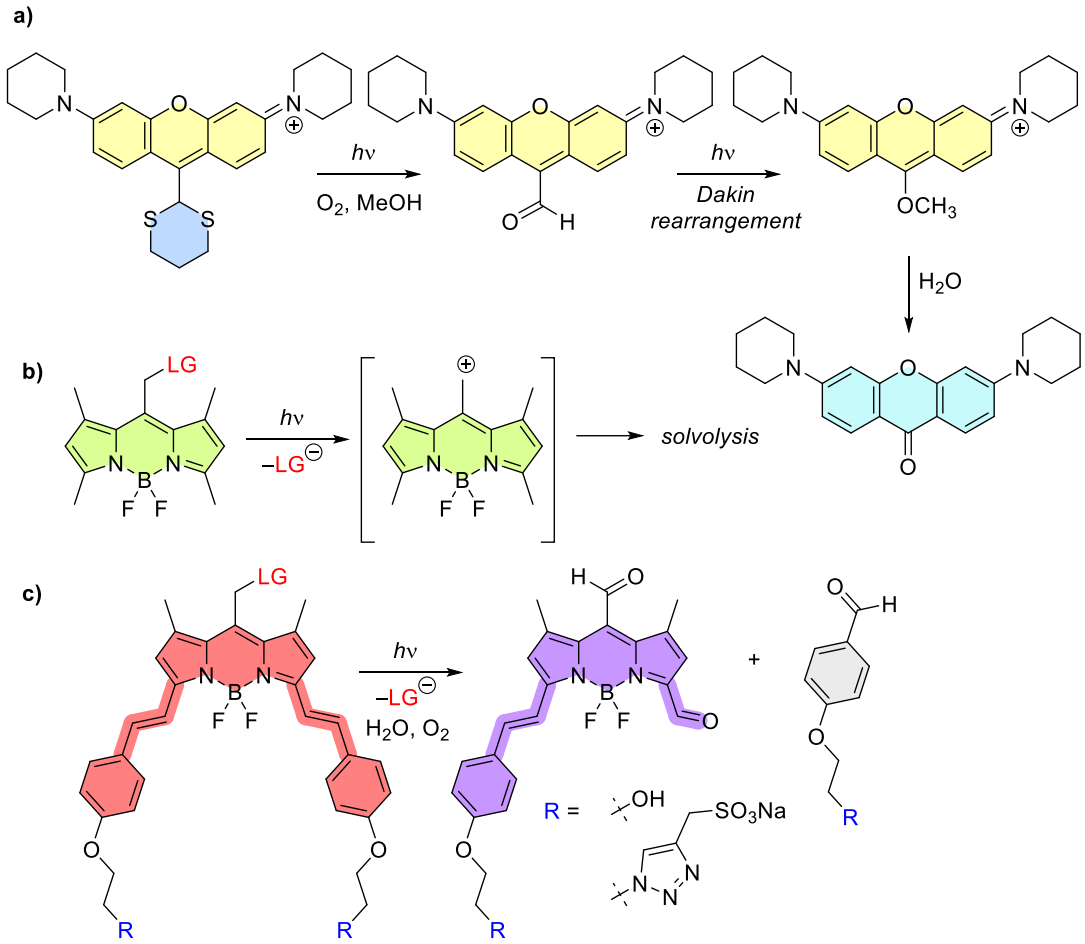

Figure 11: a) 1,3-dithianyl pyronin photochemistry, b) *meso*-methyl BODIPY photochemistry, c) BODIPY photocages for targeted delivery of signaling molecules

The field of photocages considerably changed throughout my career. I was lucky to both witness and participate in the transformation of the UV-absorbing, classical organic photocages, into advanced, yet often more limited dye-based visible light-absorbing photocages. When Professor Klán reviewed the state of the art on photocaging in 2013,[38] the only example of visible light uncaging was our fluorescein-based photocage. Seven years later, I was invited to write a follow-up, comprehensive review focused on visible-light photorelease. This *Chem. Rev.* paper covered 1,773(!) articles.[10] Since then, in less than 3 years, this review has been cited almost 300 times, clearly demonstrating that visible-light release has become a common tool for triggered release across scientific fields.

2.2. Gasotransmitter Photorelease

Releasing small molecular gases[65–68]

As is often the case in science, we began researching gasotransmitter photorelease serendipitously. When studying the fluorescein-based photocage[52] complexed with DDQ, we noticed that the photoproduct, xanthene carboxylic acid (Figure 12a), was also photochemically active. The acid decomposed to xanthenone, an analog of the photodecomposition product of 1,3-dithianyl pyronin,[55,57] and the phototransformation of the carboxylic acid to ketone involved C-C bond cleavage and loss of a C_1-containing moiety.[65] In this context, we studied two mechanistic hypotheses, photoinduced decarboxylation and photodecarbonylation.

Photodecarboxylation would lead to the formation of carbon dioxide and 9-*H* xanthene, which would further photooxidize into the final product, xanthenone. In line with this hypothesis, we confirmed that 9-*H* xanthenes efficiently oxidized to xanthenones, but xanthene carboxylic acid photodecomposed with or without oxidizing agents. Moreover, no CO_2 was detected as a byproduct. Therefore, photodecarbonylation was the only possible explanation.

To test the validity of this hypothesis, we synthesized a doubly ^{18}O-labelled carboxylic acid and performed the photoreaction in $H_2{}^{16}O$. Quantitative ^{18}O incorporation into the final xanthenone suggested that the carbonyl oxygen derived solely from the carboxylic moiety. In addition, carbonyl monoxide was the only C_1-containing photoproduct. Based on thorough mechanistic and computational studies, we concluded that photodecarboxylation occurred through the formation of α-lactone, which further decarbonylates, thus directly forming the final xanthenone.

We detected CO in the irradiated reaction mixture by complexation with hemoglobin. Carbon monoxide photorelease is highly desired in biological research of small gaseous signaling molecules – *gasotransmitters*. These gases (CO, NO, and H_2S) can transfer the signal across much longer distances than common signaling molecules as they cross the cell membrane and interact with metal-based active centres of enzymes and their cofactors. CO has vasodilatory, anti-inflammatory and wound-healing properties and bactericidal action, in addition to protecting against hypoxia.[67] Therefore, we searched for a synthetically accessible derivative with efficient carbon monoxide release, that is a photoinduced CO-releasing molecule, *photoCORM*.

Based on the *meso*-position of xantenes and BODIPYs,[54] we prepared BODIPY carboxylic acid (Figure 12b).[66] More specifically, we synthesized a series of derivatives with absorption in different regions (500 – 730 nm) and various intersystem crossing quantum yields and quantum efficiency of CO photorelease. Thanks to our collaboration with Professor Vítek, at Charles University, we were able to demonstrate the photorelease of CO *in vivo,* showing differential release of CO in different mouse tissues upon irradiation. This study demonstrated that transition metal-free photoCORM was applicable to living organisms, without any toxicity. More recently, we reviewed different photoCORMs and their properties and applications.[67]

After photoCORM, we used the BODIPY photocage as an efficient system for H_2S_n photorelease.[68] While studying BODIPY sulfonothioates, we found that sulfonates (instead of the expected sulfonothioates) are efficiently photoreleased from the system. By attaching a dansyl-sulfonothioate as a leaving group (Figure 12c), we were able to monitor the photorelease based on differences in fluorescence between the parent compound (weak fluorescence) and the irradiated mixture (strong fluorescence from both dansyl and BODIPY photoproducts). We observed this fluorogenic process in solution, on silica gel, and in U-2 OS cells, where BODIPY sulfonotioates and their photoproducts efficiently stained intracellular membranes. The photorelease was highly efficient (16%); in fact, much higher than expected from the pK_a of the leaving group.[9] The reason for this high efficiency is that, in addition to the *photosolvolysis* mechanism of *meso*-methyl BODIPY photocages, this photocage undergoes highly efficient *radical photocleavage*. This dual mechanism of photorelease is also the reason for sulfur extrusion of H_2S_n from the sulfonothioate leaving group.

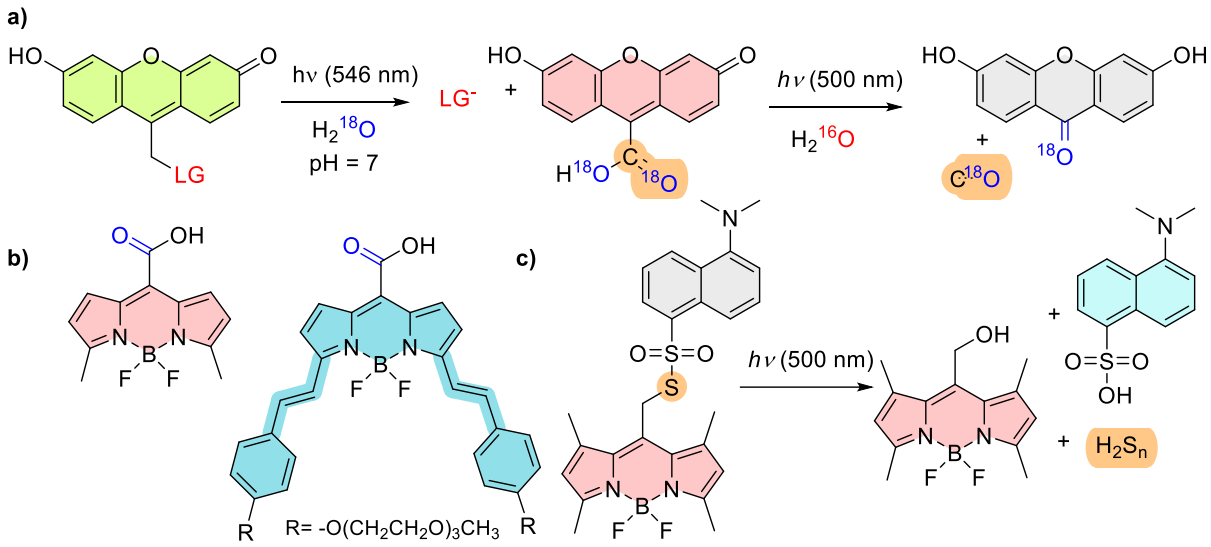

Figure 12: a) photochemical preparation and photodecarbonylation mechanism of xanthene carboxylic acid, b) BODIPY photoCORM, and c) BODIPY sulfonothioates as H_2S_n releasing molecules

2.4. Photoconjugation

Photoclick, catch and release[69,70]

Above, I described major advances in uncaging functional molecules by irradiation with visible light. Motivated by these successes in photoinduced *bond cleavage*, we also aimed at developing systems for photoinduced *bond formation*, that is, photoclick reactions. The general strategy of this process is to photochemically generate an intermediate with high ground-state reactivity with a specific substrate based on various bioorthognoal, highly efficient click reactions.[71] In collaboration with Professor Hlaváč, at Palacký University, Olomouc, we developed and studied cycloocta-1,2,3-selenadiazoles as cyclooctyne precursors, which underwent a strain-promoted azide-alkyne cycloaddition (SPAAC) reaction with azides (Figure 13a).[69] Irradiating selenadiazoles released dinitrogen and elemental selenium as photoproducts. Although this biorthogonal photoclick reaction suffered from the internal filter effect of the released colloid selenium, preventing full conversion, biotin was efficiently biorthogonally labelled for avidin-biotin systems. This study highlights the principal design approach of photoclick reactions – a precursor with protected biorthogonal functional group that can be unmasked by irradiation. This precursor should be either chromophoric or efficiently sensitized by a sensitizer.

In our following study, we asked an even more tempting research question – could we *connect* and subsequently *disconnect* two molecules only using light of various wavelengths? We named this approach *catch-and-release* and used, on the one hand, the most reliable photochemical systems known at the time – cyclopropenones (analogous to selenadiazoles, discussed above) as masked precursors of cyclooctynes formed *via* photodecarbonylation, and on the other hand, *para*-hydroxyphenacyl azide photocage as the reactive counterpart for the SPAAC reaction (Figure 13b).[70] The key design principle of this approach was the different absorption spectra of cyclopropenones and *para*-hydroxy phenacyl derivatives, which enabled us to mix all components in a solution, irradiate with 350-nm light to quantitatively *connect* the cyclopropenone and azide parts, and then switch to 313 nm to *cleave* the covalent bond between the newly formed 1,2,3-triazole moiety and the *para*-hydroxyphenacyl photocage. The *photo*-Favorskii rearrangement quantitatively produced a 4-hydroxyphenyl acetic acid derivative and a 1,2,3-*H*-triazole. This proof-of-concept study demonstrated the feasibility of *click* and *clip* reactions and their design principle,[72] which has since been developed for conjugation followed by fine-tuning of the chemical structure of conjugates.

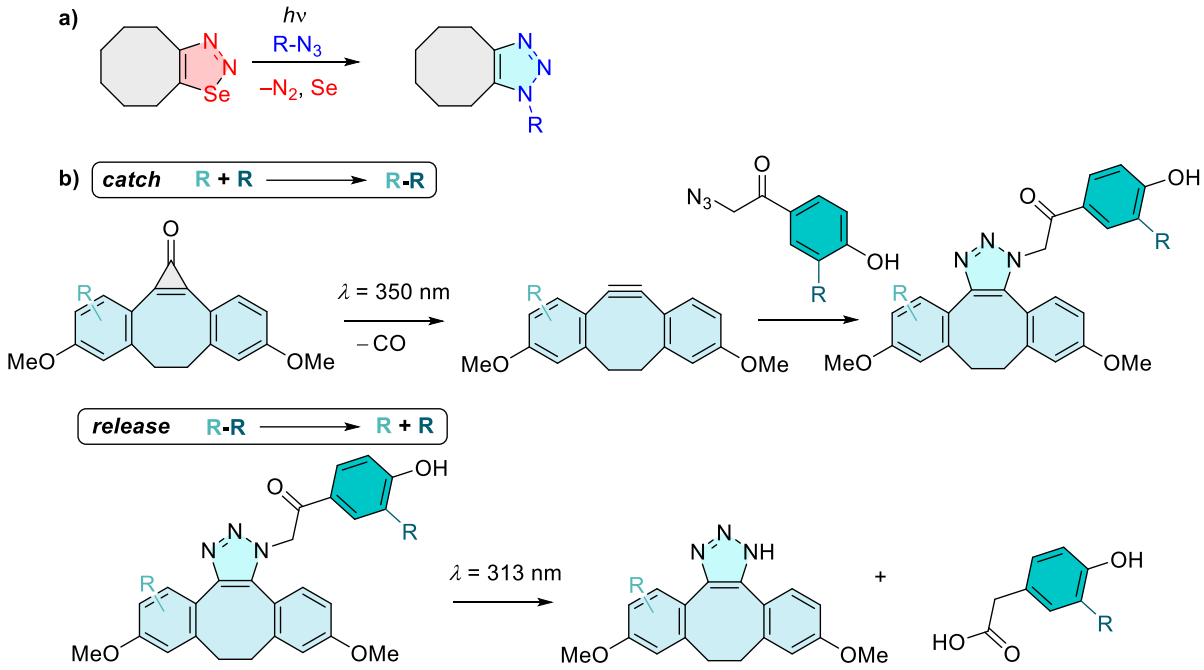

Figure 13: a) 1,2,3-selenadiazole-based photoclick reactions and b) photochemical *catch-and-release* systems

2.5. Photoswitches

Reversibly switching molecules[73–75]

Molecules that undergo reversible isomerization between two or more states upon irradiation with light at different wavelengths are known as *photoswitches*. Isomerization changes the chemical and photophysical properties of these functional molecules. This change in properties can be utilized in functional materials,[76] photochromic devices,[77] photopharmacology[78] and other biological[37] and materials applications.[79] The key properties of classical photoswitches are (i) the ability to photoswitch between two states with the highest possible conversion, e.g., near-quantitative photostationary states, and (ii) the high thermal stability of both isomers. The photostationary states are controlled by the respective forward and backward isomerization quantum yields and spectral overlap between the forms at the irradiation wavelength. Thermal stability is dictated by barriers to thermal isomerization and is often influenced by the relative (in)stability of both isomers.

In collaboration with Professor Heckel, at Goethe University, Frankfurt am Main, we synthesized and characterized a trifluoromethyl indolyl fulgide photoswitch (Figure 14a).[73] This fulgide derivative was optimized, showing excellent thermal stability of both forms, a non-cyclic *Z*-form and a cyclic *C*-form. This derivative has also been fine-tuned to minimize the spectral overlap of the respective forms for quantitative photoconversion between both forms. This unique photoswitch absorbs in the UV region and also covers the whole visible spectrum (400 – 700 nm). Therefore, we used this molecule as a chemical actinometer for visible photons.

Chemical actinometry is a method for measuring photon flux of a light source in a standardized photochemical reaction. This reaction must be reliable and robust, with well-defined and easily analyzable products. Photochemical isomerization of indolyl fulgide is accompanied by a large spectral change, enabling a simple spectroscopic determination of conversion. When characterizing the quantum yield of photoisomerization, we found an unusual relationship between this process and irradiation wavelength, that is, the quantum yield increased with the decrease in irradiation wavelength. Considering that the photoisomerization was extremely fast (~ps) and that the excited state did not have enough time to equilibrate before this isomerization, we explained this relationship by the existence of a barrier in the excited state, which is easily overcome by the hotter, higher energetic excited state of fulgide. This study addressed the need of a reliable method for measuring the photon flux of visible light sources. Since its publishing, we have sent samples of the actinometer to many laboratories in the photochemical community, which have been using it for routine calibration of their light sources (personal communication by Professor Josef Wachtveitl, Professor Pradeep Singh, Professor Manabu Abe).

Trifluoromethyl indolyl fulgide seems to be an excellent photoswitch given the high thermal stability of both forms and large spectral change associated with photoisomerization. However, its synthesis and derivatization are highly complex. For this reason, heteroazoarenes, which photoswitch between *E*- and *Z*-forms, have been introduced because they are easily synthesized and display satisfactory optical properties. Substituting their (hetero)aryl rings can not only tune the absorption spectra but also influence the thermal stability of the energetically higher *Z*-form.

We tuned the thermal stability of the *Z*-form by designing the molecules with the highest and lowest lifetime of thermal *Z*-*E* isomerization. In collaboration with Professor Venkataramani, at the Indian Institute of Science Education and Research (IISER), Mohali, India, we studied azopyrazolium photoswitches (Figure 14b).[75] These ionic compounds have excellent solubility in water and, unlike in other heteroazoarenes, hydrogen bonding interactions with water do not catalyze *Z*-*E* isomerization. This unique feature can prolong the lifetime of the *Z*-form from seconds to years. As such, azopyrazolium photoswitches are bistable in water and thus excellent candidates for photopharmacological applications.

Aiming at the opposite end of the *Z*-stability spectrum, we developed a new class of 5-phenylazopyrimidines in collaboration with Dr Procházková, at IOCB Prague. These ultrafast isomerizing photoswitches (Figure 14c)[74] showed strong push-pull character and accelerated *Z*-*E* isomerization. And given the nanosecond lifetime of the *Z*-form, these compounds emerged as excellent photochromic oscillators with possible applications in high-tech materials, ranging from advanced nonlinear optical and photorefractive materials, through photochromic optical data storage to holographic gratings. This study illustrates that even molecules such as 5-phenylazopyrimidines without observable macroscopic switching can be applied as oscillators in ultrafast-responding systems as long as the *Z*-form rapidly isomerizes back to the *E*-form.

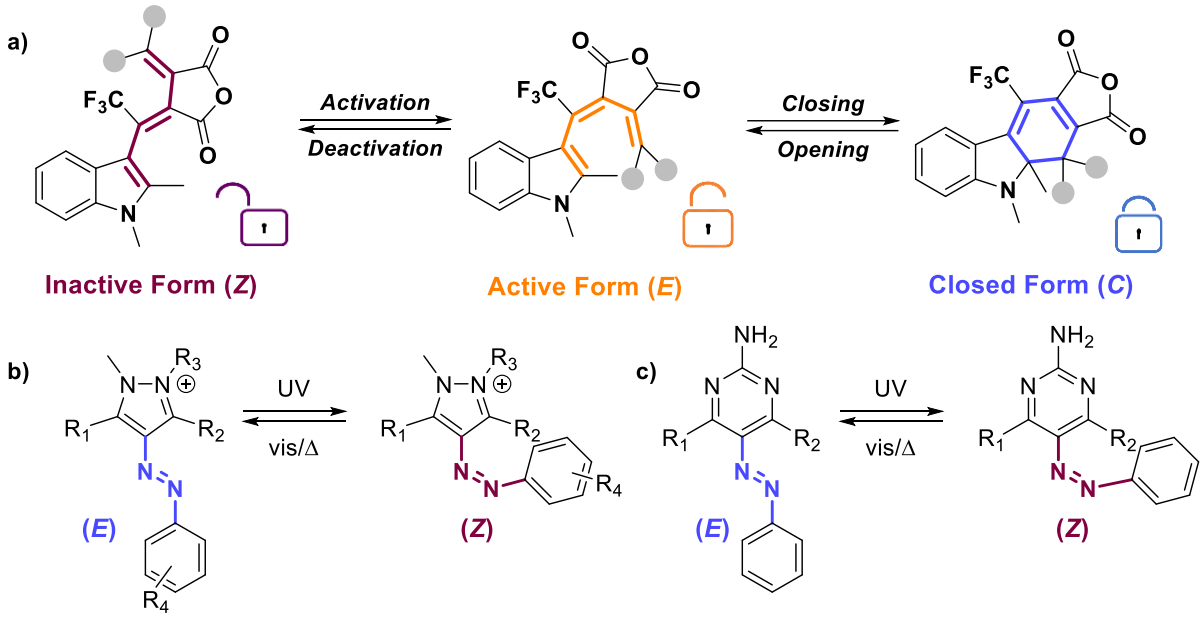

Figure 14: a) fulgide photoswitching, b) bistable azopyrazolium ionic photoswitches, c) 5-phenylazopyrimidine oscillators

(Photo)redox Transformations

Most organic molecules are *closed shell* compounds. These molecules have either doubly occupied or empty molecular orbitals in their electron configuration, so they are considered stable and hence the most commonly used thermodynamic sinks in organic reactivity. Excitation of a closed-shell molecule often results in an electron configuration with two singly occupied molecular orbitals, SOMOs. This high-energy electron and high-lying hole determine the reactivity of excited-state molecules.

Excited molecules are much stronger oxidants and reductants than their ground state analogs.[80] This property facilitates single-electron transfer between a substrate and an excited molecule (either reductive or oxidative quenching) termed *photoinduced electron transfer* (PeT). Currently, PeT is the key principle of photoredox catalysis, which uses various strongly absorbing photocatalysts capable of forming stable single-electron oxidized or reduced forms. Single-electron oxidation or reduction of organic molecules motivated us to research *open-shell* species, that is, compounds with unpaired spins. These radicals, radical ions and biradicals have unique properties and unexplored reactivity, standing out as one of the most promising lines of research in contemporary organic chemistry.

4. Fundamental Principles: Electron and Charge Transfer

Electron density transfer from an electron-rich moiety to an electron-poor area can proceed to different extents. Either *electron transfer* occurs where full charge is transferred, or a smaller, non-defined amount of electron density is transferred in a process termed *charge transfer.* The difference between these processes is blurry, especially in electron donor-acceptor (EDA) complexes[81] where charge transfer occurs in the ground state between a donor and acceptor molecule in a non-covalent complex. In these species, excitation often results in full electron transfer, forming a radical action of the donor and a radical anion of the acceptor. Charge can also be transferred in the opposite manner, involving the transfer of a proton between two functional groups, that is, between an acidic, hydrogen bond-donating site and a basic, hydrogen bond-accepting site.

4.1. Physical studies

Transferring protons[82]

In the solid phase, mixtures of acidic and basic molecules can form either a *salt*, where the proton has been fully transferred from an acid to a base, or a *cocrystal*, where the acid and base form a strong hydrogen bond, with the proton still attached to the acidic moiety. In collaboration with Dr Martin Dračínský, at IOCB, Prague, we studied proton transfer in multicomponent pharmaceutical solids with acidic and basic components, namely a model mixture of *N,N*-dimethylamino pyridine with 4-hydroxy-3-methylphenol (Figure 15a), by temperature-dependent solid-state NMR. Hydrogen transfer from the acidic phenol to the basic pyridine derivative formed charges on both components and transformed the cocrystal into a salt. This process was also observed by absorption and diffuse reflectance spectroscopy of the solid material, which showed a red-shifted charge transfer absorption band. As the temperature increased, the thermodynamically more stable salt was transformed to a cocrystal, decreasing the charge-transfer character of the mixture and the intensity of the charge-transfer absorption band. This study shows that proton transfer can be used to control charge transfer in solid mixtures and that this process does not occur as a sharp phase transition but rather a smooth shift of the positional probability of hydrogen atoms between basic and acidic moieties.

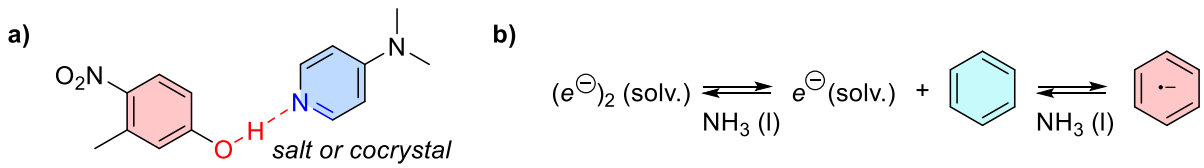

Figure 15: a) hydrogen transfer between phenols and pyridines in the solid state, b) solvated dielectron, electron and the first step of Birch reduction in liquid ammonia

Solvated electrons[83]

When detaching from a molecule, an electron is released to the solvent, forming a *solvated electron*. Depending on the stabilizing and solvating properties of the solvent, the lifetime of such a species can vary from microseconds to hours. Some protic, Brønsted acidic solvents, such as water, quickly react with electrons, forming hydrogen. Basic solvents can however create a persistent solvation sphere that prevents the electron from reacting.

Liquid ammonia is one of the most stabilizing solvents for solvated electrons. Ammonia stabilizes electrons to such an extent that, at high concentrations (> 1 mM), solvated dielectrons can be formed in this solvent.[84] The famous blue color of solvated electrons in ammonia was discovered by Humphry Davy at the beginning of 19th century.[85] Since then, solvated electrons have been used in various reactions, particularly Birch reduction of arenes.[86] In collaboration with Professor Jungwirth, at IOCB, Prague, we characterized the key intermediates of the Birch reduction process – the solvated electron and dielectron and the benzene radical anion (Figure 15b).[83] We used two seemingly unrelated methods, cyclic voltammetry and photoelelectron spectroscopy. Aided by electronic structure calculations, we quantified the electron-binding energies and the studied species, using Birch reduction as a case study to directly connect *ionization potenials*, measured by photoelectron spectroscopy, with *reduction potentials*, determined by voltammetry. The results showed that solvated dielectrons are weaker reductants than solvated electrons and that the reduction potential of benzene lies between these two values. Therefore, at high electron concentrations, benzene reduction to the corresponding radical anion is hindered by the formation of solvated dielectrons. This study highlights the potential of solvated electron chemistry because stabilizing these species enables us to leverage their unique reduction properties.

4.2. Stable Radical Ions

Single electron reduction[87–89]

Attaching a solvated or photoexcited electron to a closed-shell molecule creates a corresponding singly reduced species. Depending on the initial charge of the closed-shell molecule (neutral, cation, and dication), the reduced species can be radical anion, radical, and radical cation, respectively. A general rule of thumb is that positively charged molecules are good electron acceptors. Below, I discuss the following examples of redox-active molecules with increasing demands for reduction, which also reflects the gradual decrease in stability and increase in reactivity of the singly reduced species.

In collaboration with Professor Vladimír Šindelář, at Masaryk University, Brno, we studied the complexation of dicationic methyl viologen (MV) into dodecamethylbambus[6]uril (BU6) macrocyle (Figure 16a).[87] MV and BU6 form cocrystals with alternating MV and BU6 layers. When irradiating these crystals with UV light, electrons were transferred from the BU6 macrocyclic cage to the dicationic MV, forming MV radical cations with a blue hue. These blue crystals remained stable to air, even though the reduced methyl viologen alone would be rapidly oxidized by oxygen. We explained this unusual stability of reduced MV by the limited

diffusion of oxygen within the confined environment of the crystalline material. Heating the blue material resulted in back electron transfer, restoring the initial state, accompanied by loss of color of the crystals. This study demonstrates that radical ions can be stabilized by confining them into supramolecular complexes, thereby preventing them from engaging in other bimolecular interactions.

Preventing a radical ion from establishing bimolecular interactions is an efficient way of stabilizing them but precludes its use as a reagent or catalyst, so alternative strategies must be applied to stabilize radicals and radical ions. Most redox-active (photo)catalysts have been optimized to efficiently produce radical ions. Their properties are crucial for specific reactivity, yet their detection in (photo)catalytic reaction mechanisms often eludes chemists. Therefore, synthesizing radical ions derived from common catalysts and studying their stability and properties helps to design novel catalytic reactions.

Based on a study by Dr Indrajit Ghosh, at the University of Regensburg, Germany, reporting chromoselective photocatalytic reduction – using different color of light to irradiate a reaction mixture containing rhodamine 6G as the photocatalyst to yield different photoreaction products –,[90] we prepared a rhodamine 6G radical and studied its properties and stability (Figure 16b).[88] When irradiated, rhodamine 6G radical formed solvated electrons collected by a spectroelectrochemical electrode, rendering rhodamine 6G an excellent source of solvated electrons with a reduction power matching that of alkali metals. Accordingly, detailed studies of radical ions can reveal novel properties, opening up opportunities for developing unexpected applications.

Photocatalysts such as rhodamine 6G must efficiently generate radical anions for tens to hundreds of catalytical cycles, but dyes in solar cells must be reduced and re-oxidized without decomposition for millions of cycles. For this reason, photovoltaic applications require much more stable dyes. One of the dyes most commonly used as a non-fullerene acceptor material in organic photovoltaics is perylene diimide. Perylene diimide forms a stable radical anion, and its thermal and photostability surpass that of most other organic chromophores. In collaboration with Professor Trimmel, TU Graz, we prepared a series of perylene diimides functionalized with Si and Ge in the bay region (Figure 16c)[89] and found that semimetal substitution induced a red shift in absorption. After assessing the performance of these dyes as acceptors in organic photovoltaics, we determined that germanium-substituted perylene diimide in combination with the electron-donating polymer PM6 reached a high power conversion efficiency of 5% thanks to the high electron mobility in the absorber layers and high crystallinity of the material. This study shows that optimizing the derivatization of chromophores that form a stable radical anion fosters the development of advanced, high-performing acceptor materials for organic photovoltaics.

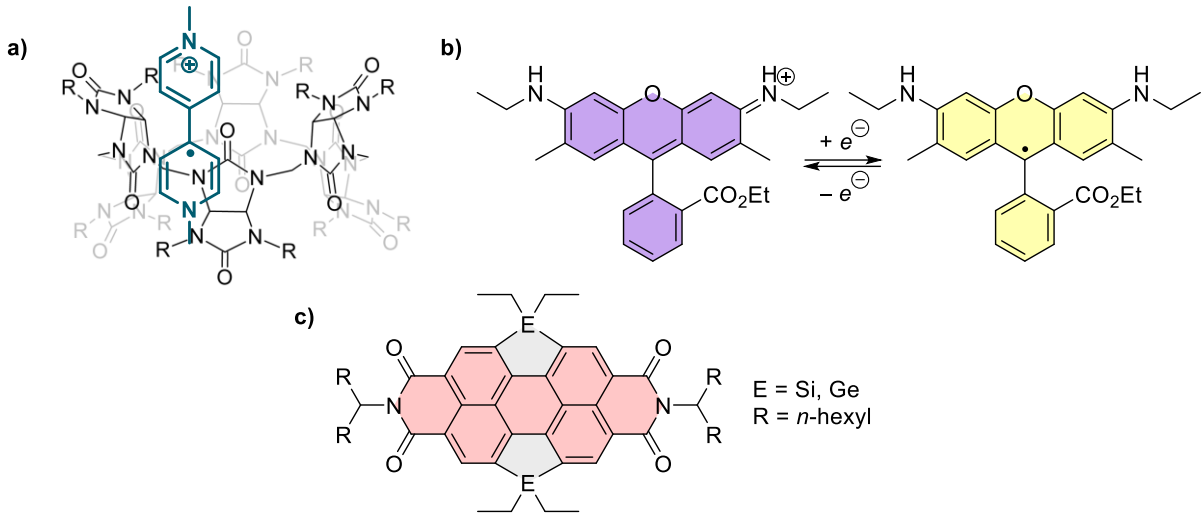

Figure 16: a) MV and BU6 structure, b) rhodamine 6G radical, c) Si- and Ge-substituted PDI derivatives

Radical cation reactivity[91]

We primarily studied organic radicals and radical ions as intermediates of redox and catalytic reactions. When analyzing triarylamminium radical cations, common organic synthesis oxidants, we noticed their unique reactivity, so we focused on commercially available *tris*(4-bromophenyl)aminium hexachloroantimonate, also known as magic blue (MB). When mixed with silanes, MB catalytically deprotects *tert*-butyl group from the corresponding esters, ethers, carbonates and carbamates (Figure 17a).[91] This reactivity is enabled by the Lewis acidity of triarylamminium radical cations. Consequently, MB coordinates to the carbonyl group of the *tert*-butyl ester (Figure 17b) and facilitates isobutene cleavage and subsequent formation of silylester, which is further hydrolyzed to the final free carboxylic acid.

This unexpected reactivity prompted us to screen triarylamminium radical cations for other reactivity modes. The results showed that they act as excellent catalysts in aromatization reactions, hydrogen atom abstractions and C-C bond-forming reactions at the α-position of ethers. Accordingly, removing one electron from a formerly Lewis basic triarylamine creates a species with umpolung reactivity suitable for various organic reactions.

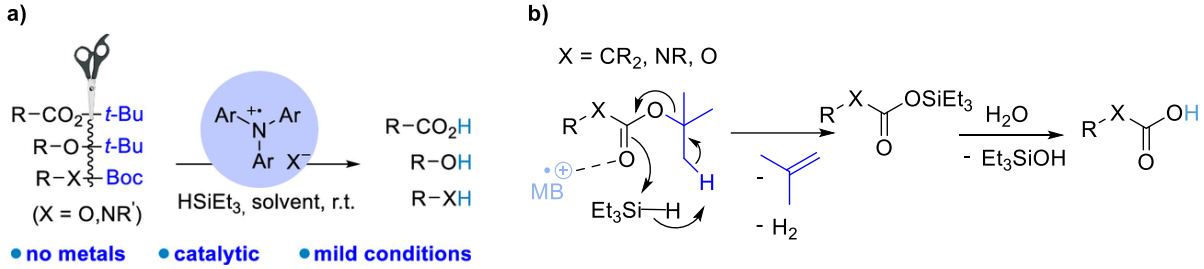

Figure 17: a) catalytic activity of magic blue for de-*tert*-butylations of esters, ethers, carbonates and carbamates, b) deprotection mechanism

5. Electron Transfer in Reaction Methodology

Open-shell compounds not only have unique properties but also play key roles in photochemical reactions as reactive intermediates, reduced or oxidized photocatalysts and excited states with high multiplicity. In principle, open-shell molecules can be generated by light in two ways: by (i) photo or redox-sensitized homolytic fission of reactive starting materials and by (ii) photoinduced electron transfer from/to a photocatalyst, leading to cascade of redox, radical, and covalent processes.

5.1. Photogeneration of Reactive Intermediates

Photochemical fluoroalkylation[92,93]

In collaboration with Dr Ullrich Jahn, IOCB Prague, we studied the photochemical C(sp^3)-H amination at the α-position of readily available and commercial feedstock ethers, using nonaflyl azide as the amination reagent (Figure 18a).[92] UV irradiation excited the nonaflyl azide, leading to dinitrogen extrusion and the formation of *N*-nonaflyl nitrene. This nitrene further reacted with the α-position of ethers, forming the aminated product. The quantum yield of the reaction was ~500, indicating that the radical chain mechanism was efficient, that light was used only to initiate the radical chain process, and that molecules with weak chemical bonds tend to break these bonds upon excitation. Therefore, photogenerated reactive intermediates can be leveraged for novel synthetic reactions.

In a similar study in collaboration with Dr Petr Beier, IOCB Prague, we analyzed direct excitation of fluoroalkylated cyclic λ^3-iodanes, which efficiently generated a fluoroalkyl radical. This radical reacts with electron-rich aromatic residues of amino acids, such as phenylalanine, tyrosine, and histidine.[93] Tryptophane showed the highest reactivity, preferentially so at position 2 of the pyrrole ring (Figure 18b). The reaction mechanism proceeded through a long-lived radical chain, even tens of minutes after switching off the light. The reaction was initiated by blue light, which excited cyclic λ^3-iodanes into a dissociative state, cleaving off the fluoroalkylated radical. This study shows that low-energy visible light can induce the dissociative cleavage of compounds with tail absorption in this region. With an efficient radical chain mechanism, this reaction is high yielding and relatively fast, despite the low probability of formation of the initial fluoroalkylated radicals.

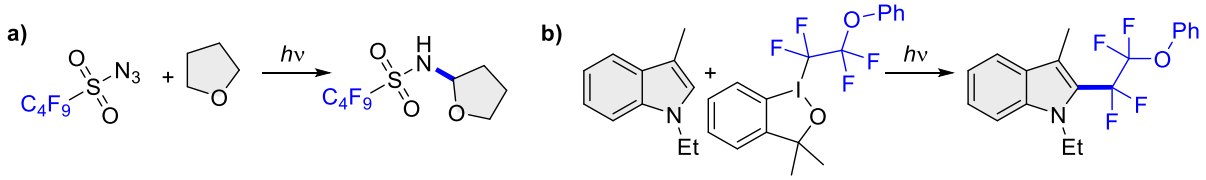

Figure 18: a) photochemical amination of ethers, b) trifluoroalkylation of tryptophan in a peptide.

5.2. Photoredox Reactivity

Photoredox catalysis has rapidly grown in the last two decades, yielding a plethora of novel synthetic transformations and revolutionizing how we look at radical reactivity. Thanks to its low requirements for instrumentation, photocatalysis stopped being an exclusive domain of photochemists and has now spread to many organic synthesis laboratories.[94] The most important component of photocatalytic reactions is the photocatalyst, a molecule that efficiently absorbs visible light. The photocatalyst has a long-lived excited state that enables electron and energy transfer reactions. When excited, the photocatalyst becomes a stronger reductant and oxidant and, therefore, two modes of photoredox catalysis are possible, namely reductive and oxidative quenching. *Reductive quenching cycle* involves the reduction of the excited photocatalyst by a suitable electron donor, followed by re-oxidation by a substrate or terminal oxidant. *Oxidative quenching cycle* is exactly the opposite – the excited photocatalyst transfers an electron onto a substrate and gets reduced back by a reductant molecule to close the catalytic cycle. Most organic photocatalysts were fine-tuned to be both strong oxidants and strong reductants in the excited state,[95] so both oxidative and reductive quenching cycles are almost equally probable in photocatalytic mechanisms. Only a detailed mechanistic study can reveal the operating mode of the photoreaction.

We began our photocatalysis research in collaboration with Prof. Burkhard König, at University of Regensburg, a leading expert in this field. In addition to developing novel reaction methods, our main aim was to elucidate photocatalytic reaction mechanisms. When I entered the field of photocatalysis in 2012, many studies had only developed organic methods without proposing any mechanisms. This oversight led to many misconceptions in the design of photoredox catalytic systems, which are only now being slowly abolished from the literature. The main problem of early photocatalytic studies was the low reproducibility and transferability of reaction methods between different laboratories. Each lab used a different light source, often polychromatic, exciting not only the photocatalyst but also the substrates. Furthermore, the geometry of each setup was different. Most photocatalytic reactions were complex mixtures of many components (substrates, photocatalysts, sacrificial electron donors/ acceptors, other additives) mixed at a high concentration. This optically dense mixture was irradiated with a relatively weak light source, thus irradiating only small volume of the reaction mixture. All these factors contributed to the chasm between the 'real world of the organic photocatalytic reactions' and the simulated, precisely defined conditions of photophysical experiments aimed at elucidating reaction mechanisms.

To bridge this chasm, we developed a general strategy for describing photocatalytic reactions and studying their mechanisms, including characterizing the light source (spectral profile, photon flux, and intensity fluctuations), concentration effects (steady state quenching and photocatalyst complexation with substrates), and quantum yields (wavelength variation, light intensity variation, and control of radical chain processes). In addition, carefully designing control experiments (omitting one of the components of the catalytic system) can provide important insights about the role of each reagent. As mentioned above, photocatalytic mechanisms can proceed through either oxidative or reductive quenching cycle. To distinguish them, we developed a quenching technique[96] measuring the luminescence of the photocatalyst

in presence of the substrate and other reaction components. Efficient luminescence quenching indicates electron or energy transfer from/ to an excited photocatalyst. Moreover, detecting a radical cation or radical anions by transient absorption spectroscopy and open shell species by electron paramagnetic resonance and comparing them with spectroelectrochemically generated single-electron oxidized/ reduced species can further support and refine the final proposed mechanism.

In this context, we studied various photocatalytic reactions, which I categorized according to the final chemical output as *photoreductions*, *photooxidations,* and *covalent bond formation* reactions. However, this classification does not necessarily mean that photoreductions proceed through reductive quenching cycles, for example. Each photoredox mechanism is specific and must be evaluated individually.

Photoreductions[97,98]

In our first study, we developed a chemoselective photocatalytic reduction of aldehydes by rhodium(III) hydride.[97] For this purpose, we used triethanolamine as the sacrificial electron donor, proflavine as the photocatalyst and [Cp*Rh^{III}(bpy)Cl]Cl as the electron mediator (Figure 19a). Thanks to the slow photochemical *in situ* generation of the reducing rhodium-based hydride, we achieved a high reduction chemoselectivity. By detailed analysis of the photocatalyst, we found that proflavine reacts by ionization coupled with oxidative quenching from the singlet excited state and by reductive quenching with triethanolamine from the triplet state. As such, proflavine stands out as one of the few examples of a photocatalyst whereby both reductive and oxidative quenching cycles operate simultaneously and lead to the desired product.

Some excited photocatalysts have high reduction potentials, which are further increased by a second excitation of the singly reduced photocatalyst. This *consecutive photoinduced electron transfer* (conPeT)[99] leads to the excited dublet states with extreme reducing power. However, the lifetime of such species lies in the picosecond range, precluding bimolecular interactions with substrates. For this reason, we used dysprosium(III) ions as electron mediators for metal-ion-coupled electron transfer combined with conPeT of rhodamine 6G.[98]

The excited state of rhodamine 6G is reductively quenched by diisopropylethylamine, forming rhodamine radical as a complex with Dy^{III} salt. This complex is further excited and dissociates to form a highly reducing Dy^{II} salt. This reduced electron mediator reduces aryl chlorides, forming aryl radicals that abstract hydrogen and form plane arenes (Figure 19b). Combined, these findings demonstrate that a mediator can be used to harvest the extreme reduction potential of the excited state of radical ions.

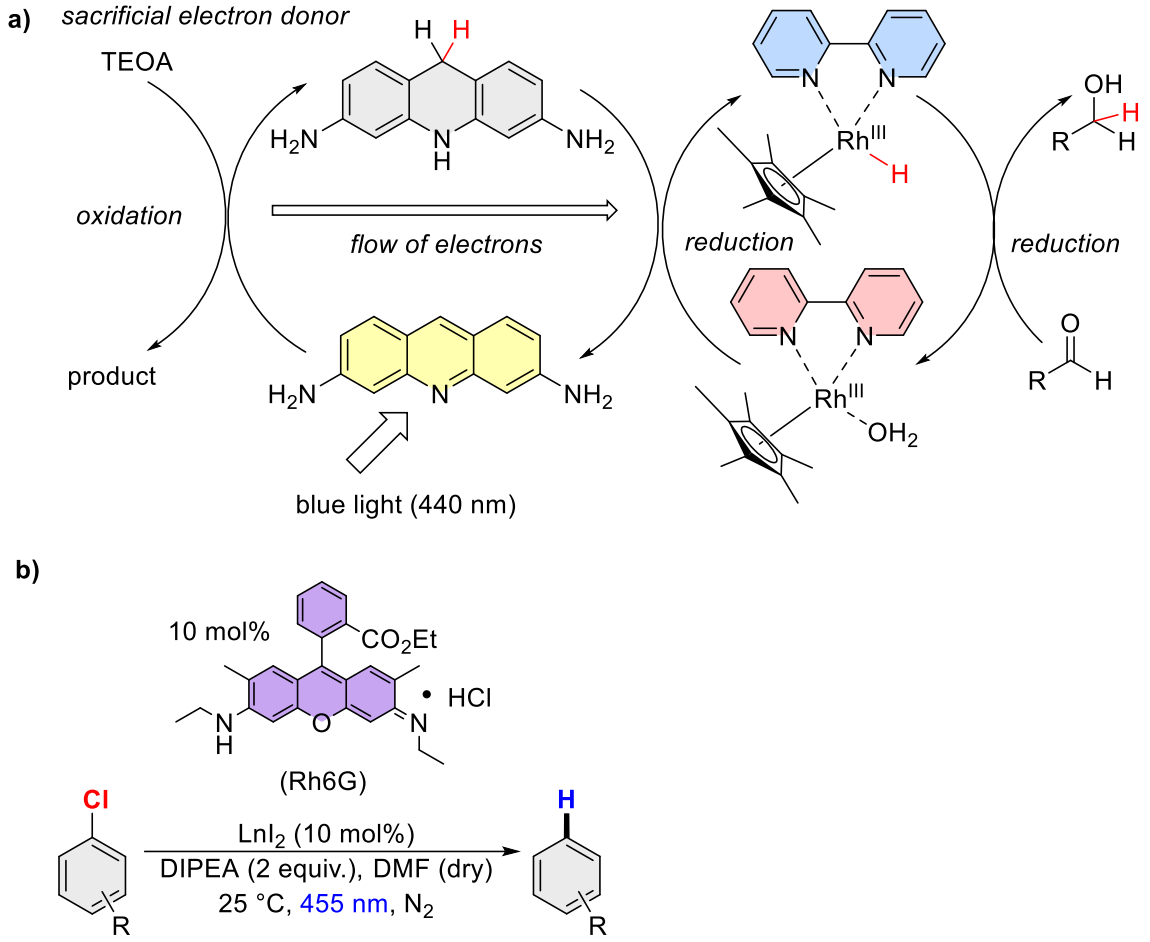

Figure 19: a) rhodium-catalyzed chemoselective reductions of aldehydes in the presence of ketones and b) lanthanide-mediated dehalogenation of electron-poor arenes. Ln = lanthanide.

Photooxidations[100,101]

Photoredox catalysis can generate highly reactive intermediates with unique reactivity. As a case in point, we have photocatalytically generated the nitrate radical ($NO_3\cdot$) by oxidating nitrate salts with mesityl acridinium excited by visible light (Figure 20a).[100] The acridinium photocatalyst was reductively quenched from its singlet excited state and formed an acridinyl radical with a characteristic absorption spectrum. The acridinyl radical was further re-oxidized by oxygen. The resulting $NO_3\cdot$ reacted with aromatic alkynes, a previously well-studied model reaction of $NO_3\cdot$, and was also used to oxidate alcohols to ketones. Even though the nitrate radical was never detected or accumulated in the reaction mixture, its reactivity was high enough to efficiently oxidize the alkyne and alcohol substrates.

Oxidation reactions can be accomplished without oxygen or any other added terminal oxidant, as shown in collaboration with Professor Radek Cibulka, at UCT Prague. In this study, we developed a mild chemoselective oxidation method for converting alcohols to ketones using deazaflavinium salts as photocatalysts (Figure 20b).[101] The reaction in degassed acetonitrile with a low catalyst loading (8 mol%) produced quantitative yields of oxidized products, proceeding as an unprecedented anaerobic dehydrogenation of alcohols using acetonitrile as terminal oxidant. Through precise transient absorption spectroscopy measurements, we

demonstrated the presence of acetonitrile radical anion and its dimer in the irradiated reaction mixture. The reduced acetonitrile further underwent hydrogen atom transfer, proton transfer and hydrolysis to acetaldehyde, which was detected by ^{1}H NMR as a hydrazone. The main advantage of this photooxidation over existing methods is the absence of reactive oxygen species, which are otherwise generated in the presence of oxygen. Therefore, photooxidation enables the chemoselective oxidation of alcohols to ketones in the presence of sulfides, which remain intact.

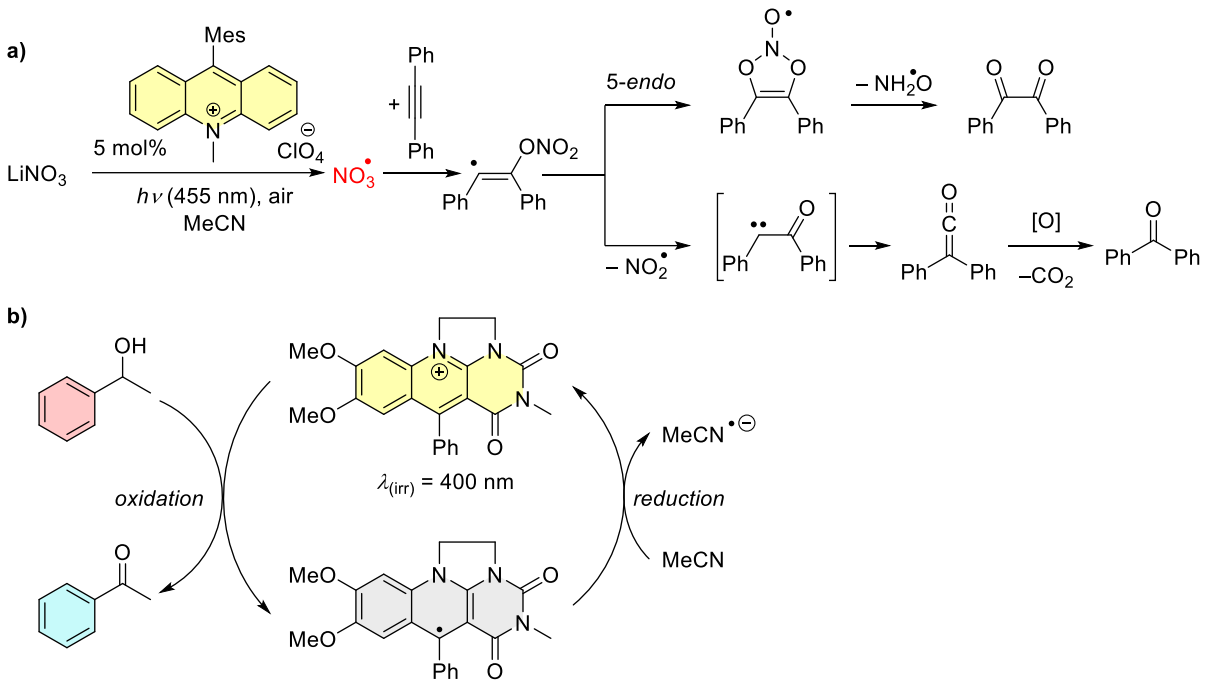

Figure 20: a) photooxidation of nitrate anions to $NO_3\cdot$ and b) chemoselective oxidation by deazaflavinium salts

Covalent Bond Formation[96,102–104]

Photoredox catalysis is based on reductions and oxidations of various substrates, but its overall scope is not necessarily limited to redox reactions. Many substrates are activated by a single-electron transfer, reacting with other molecules and thus forming covalent bonds. In our previous studies, we have reported on the photocatalytic formation of single or multiple C-C, C-S, C-N bonds by visible light-driven photocatalysis.

In collaboration with Burkhard König, at University of Regensburg, we found that eosin Y undergoes efficient reductive quenching by triethylamine, forming the respective radical anion. This highly reducing species transfers an electron to pentafluorobromobenzene, which expels bromide anion and forms a pentafluorophenyl radical (Figure 21a).[102] This radical further adds to (hetero)arenes, forming biaryls and can be even used for late-stage functionalization of complex natural products, such as alkaloid brucine.

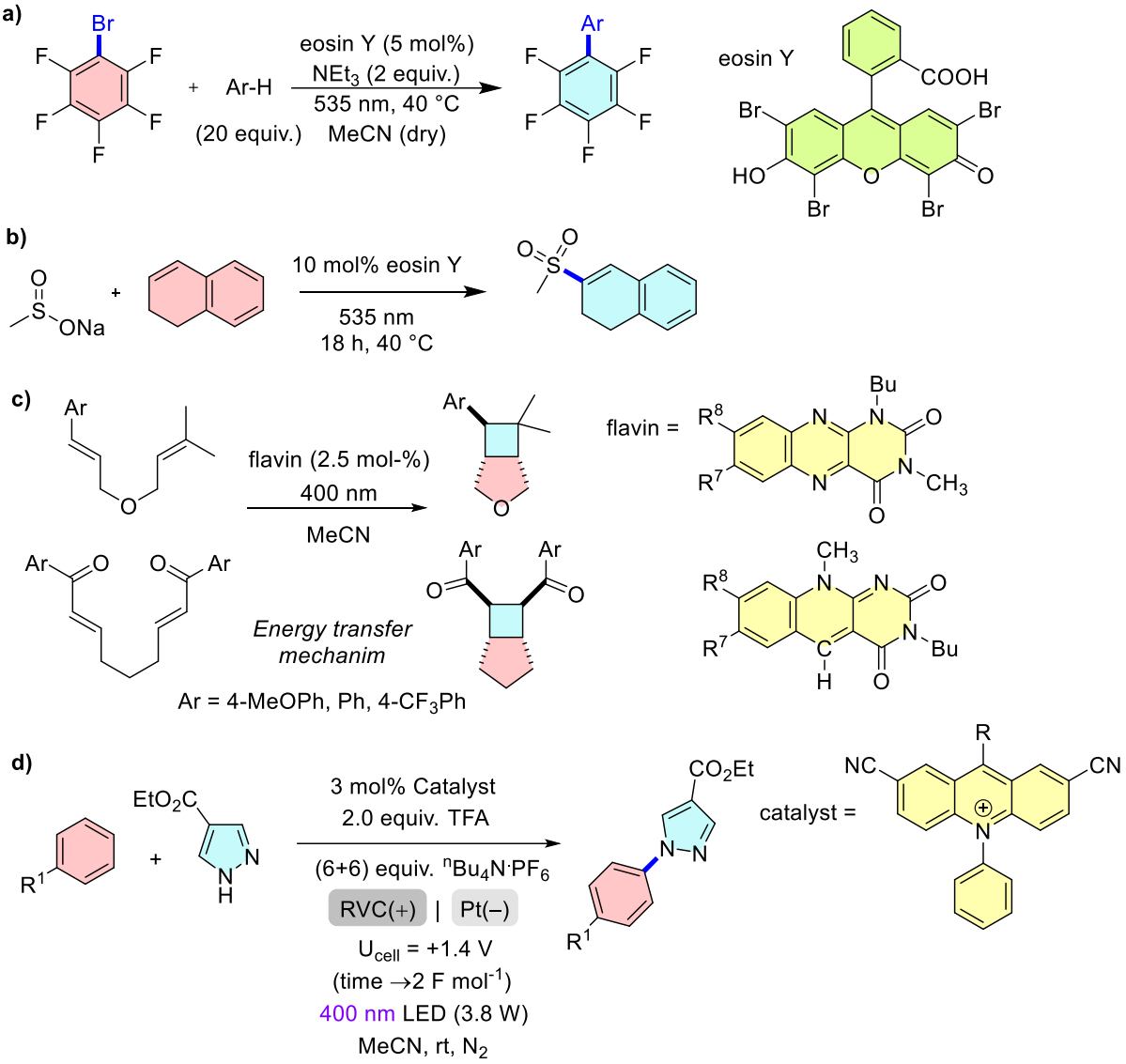

Figure 21: a) perfluoroarylation of arenes, b) sulfonylation of alkenes, c) cycloaddition reactions and d) acridinium-catalyzed arylation reactions, RVC = reticulated vitreous carbon

As a universal catalyst, eosin Y can be also used in the oxidative quenching cycle. Excited eosin Y donates one electron to nitrobenzene, a sacrificial oxidant, forming the respective radical cation, which oxidizes sulfinate salts to S-centered radicals (Figure 21b).[96] These radicals add to double bonds of styrenes, forming vinyl sulfone products. Both these studies show that, when combined with a powerful sacrificial electron acceptor or donor, organic photocatalysts can act as strong oxidant and reductants, respectively. This property can be used to generate radical intermediates that selectively react with alkenes and arenes.

So far, we have only discussed photoredox catalysts that undergo photoinduced electron transfer processes. However, excited photocatalysts can also transfer energy onto substrates. In particular, excited triplet states are efficient photosensitizers and can be used to drive photochemical processes. In our study, in collaboration with Prof. Cibulka, at UCT Prague, we used flavine analogs, deazaflavins and alloxazines as efficient triplet photosensitizers for intramolecular cyclization of substituted styrene dienes and bis(aryl enones) to the corresponding cyclobutanes (Figure 21c).[103] Excited flavine analogs underwent efficient

intersystem crossing to the triplet state, transferred energy to the diene substrate and promoted the thermally forbidden [2+2] cycloaddition reaction. This study shows that photosensitization can be used not only to produce singlet oxygen (*vide supra*) that destroys all molecules in the surrounding environment but also to induce productive reactions, forming covalent C-C bonds.

The most challenging mechanistic study of my entire career involved electron-poor acridones as catalysts for C-H azolation of PhCl (Figure 21d).[104] Combining photocatalysis and electrolysis in an electro-activated photocatalysis setup led to efficient pyrazole coupling of pyrazoles with electron poor arenes. Developed in collaboration with Dr Joshua Barham, at University of Regensburg, the chemical yields and substrate scope were high, which enabled us to elucidate the elusive reaction mechanism. We found that the excited state of acridone was not being quenched by any substrate and it lacked an oxidation potential high enough to oxidize the substrates. After extensive research, we realized that acridone acted as a pre-catalyst and was transformed into an acridinium analog in the presence of Brønsted acid and a platinized electrode with an applied potential. This acridinium had a much higher oxidation power and efficiently catalyzed the reaction but was photochemically unstable, requiring constant re-supplying from the acridone precursor during the reaction. This study illustrates how redox active chromophoric molecules deemed photocatalysts can transform into catalytically active species with completely different redox and spectroscopic properties during a reaction.

Conclusion and Future Perspectives

Organic molecules often display a unique and unexpected reactivity in their excited states and their excited-state behavior often contrasts with their ground-state chemistry. Accordingly, guidelines with predictive power must be formulated to rationally design photochemical systems. Advancing the fundamental understanding of excited-state dynamics, our research findings have helped us reformulate and further specify such guidelines about various phenomena, including Kasha's rule, hydrogen and electron transfer, heavy-atom effect and others. Beyond excited states, we have studied open shell species, such as radicals and radical ions, identifying new modes of ground-state and photochemical reactivity of these transient species. The results of our fundamental research have led to the development of reaction methods, including new synthetic transformations leveraging photoinduced and redox activation of catalysts and substrates.

In the last decade, our research has focused on functional molecules, mainly photocages, photoswitches and photoconjugation molecules. During this period, we have developed new types of these compounds, using chemical structures outside mainstream research, optimizing their properties and function and developing new modes of activation. In doing so, we have contributed to the rapid growth of these research areas, especially photoredox catalysis, visible light photoactivation and photopharmacology.

In our current research, we are going one step further, using *functional molecules* for *functional systems*. Among our key lines of research, we are exploring and exploiting novel modes of photoinduced chemical reversibility. Concomitantly with a precise control over geometry and absorption properties, we strive to develop systems for reversible photochemical

covalent bond formation and cleavage and for reversible photoinduced electron transfer. These systems may be applied in light-responsive materials, novel types of solar cells and rechargeable batteries, and fluorescent labelling, oligonucleotide function control, proteomics, photopharmacology, medicinal chemistry and diagnostics.

In conclusion, the field of photochemistry has a tremendous potential for breakthrough discoveries. Only now have we reached a point where our theory and methods (e.g., computations) for excited-state processes are finally useful as their high predictive power can be used to rationally design complex photochemical systems with unprecedented functionality. But the time when we will be able to fulfil the potential of light is yet to come.

References

[1] A. S. Travis, *Technol. Cult.* **1990**, *31*, 51–82.
[2] "In the beginning Were the Dyes," can be found under https://www.basf.com/global/en/who-we-are/history/130-years-of-basf-in-china/how-it-all-began/in-the-beginning-were-the-dyes.html, **n.d.**
[3] C. Cooksey, *Biotech. Histochem.* **2017**, *92*, 506–512.
[4] G. G. Stokes, *Philos. Trans. R. Soc. Lond.* **1997**, *142*, 463–562.
[5] *Maurice Ceresole*, **1891**, US456081A.
[6] R. B. Mujumdar, L. A. Ernst, S. R. Mujumdar, C. J. Lewis, A. S. Waggoner, *Bioconjug. Chem.* **1993**, *4*, 105–111.
[7] D. Frackowiak, *J. Photochem. Photobiol. B* **1988**, *2*, 399.
[8] A. Jablonski, *Nature* **1933**, *131*, 839–840.
[9] T. Slanina, P. Shrestha, E. Palao, D. Kand, J. A. Peterson, A. S. Dutton, N. Rubinstein, R. Weinstain, A. H. Winter, P. Klán, *J. Am. Chem. Soc.* **2017**, *139*, 15168–15175.
[10] R. Weinstain, T. Slanina, D. Kand, P. Klán, *Chem. Rev.* **2020**, *120*, 13135–13272.
[11] T. Slanina, R. Ayub, J. Toldo, J. Sundell, W. Rabten, M. Nicaso, I. Alabugin, I. Fdez. Galván, A. K. Gupta, R. Lindh, A. Orthaber, R. J. Lewis, G. Grönberg, J. Bergman, H. Ottosson, *J. Am. Chem. Soc.* **2020**, *142*, 10942–10954.
[12] Kekulé, August, *Bull. Société Chim. Paris* **1865**, *3*, 98–110.
[13] E. Hückel, *Z. Für Phys.* **1931**, *70*, 204–286.
[14] P. von R. Schleyer, *Chem. Rev.* **2001**, *101*, 1115–1118.
[15] H. Ottosson, *Chem. Sci.* **2023**, *14*, 5542–5544.
[16] L. Kaplan, J. S. Ritscher, K. E. Wilzbach, *J. Am. Chem. Soc.* **1966**, *88*, 2881–2882.
[17] D. Dunlop, L. Ludvíková, A. Banerjee, H. Ottosson, T. Slanina, *J. Am. Chem. Soc.* **2023**, *145*, 21569–21575.
[18] H. Xin, X. Gao, *ChemPlusChem* **2017**, *82*, 945–956.
[19] L. Ruzicka, A. J. Haagen-Smit, *Helv. Chim. Acta* **1931**, *14*, 1104–1122.
[20] P. Bakun, B. Czarczynska-Goslinska, T. Goslinski, S. Lijewski, *Med. Chem. Res.* **2021**, *30*, 834–846.
[21] J. Michl, E. W. Thulstrup, *Tetrahedron* **1976**, *32*, 205–209.
[22] M. Kasha, *Discuss. Faraday Soc.* **1950**, *9*, 14.
[23] K. Jorner, W. Rabten, T. Slanina, N. Proos Vedin, S. Sillén, J. Wu Ludvigsson, H. Ottosson, P.-O. Norrby, *Cell Rep. Phys. Sci.* **2020**, *1*, 100274.
[24] J. Yan, T. Slanina, J. Bergman, H. Ottosson, *Chem. – Eur. J.* **2023**, *29*, e202203748.
[25] W. F. Meggers, F. J. Stimson, *JOSA* **1920**, *4*, 91–104.
[26] F. H. Quina, G. T. M. Silva, *J. Photochem. Photobiol.* **2021**, *7*, 100042.
[27] N. J. Turro, *Modern Molecular Photochemistry*, University Science Books, **1991**.
[28] F. H. Quina, in *Chem. Biol. Gener. Excit. States* (Eds.: W. Adam, G. Cilento), Academic Press, San Diego, **1982**, pp. 1–36.
[29] R. L. Lipson, E. J. Baldes, A. M. Olsen, *J. Natl. Cancer Inst.* **1961**, *26*, 1–11.
[30] R. L. Lipson, E. J. Baldes, A. M. Olsen, *J. Thorac. Cardiovasc. Surg.* **1961**, *42*, 623–629.
[31] D. Kessel, *J. Clin. Med.* **2019**, *8*, 1581.
[32] J. A. Anshori, T. Slanina, E. Palao, P. Klán, *Photochem. Photobiol. Sci.* **2016**, *15*, 250–259.
[33] E. Palao, T. Slanina, P. Klán, *Chem. Commun.* **2016**, *52*, 11951–11954.
[34] M. Poljak, L. Wohlrábová, E. Palao, J. Nociarová, J. Míšek, T. Slanina, P. Klán, *Chem. Commun.* **2022**, *58*, 6389–6392.

[35] N. Ankenbruck, T. Courtney, Y. Naro, A. Deiters, *Angew. Chem. Int. Ed Engl.* **2018**, *57*, 2768–2798.
[36] A. C. Kneuttinger, *Biol. Chem.* **2022**, *403*, 573–613.
[37] W. Szymański, J. M. Beierle, H. A. V. Kistemaker, W. A. Velema, B. L. Feringa, *Chem. Rev.* **2013**, *113*, 6114–6178.
[38] P. Klan, T. Solomek, C. G. Bochet, A. Blanc, R. Givens, M. Rubina, V. Popik, A. Kostikov, J. Wirz, *Chem. Rev.* **2013**, *113*, 119–191.
[39] P. Klán, T. Šolomek, C. G. Bochet, A. Blanc, R. Givens, M. Rubina, V. Popik, A. Kostikov, J. Wirz, *Chem. Rev.* **2013**, *113*, 119–191.
[40] J. A. Barltrop, P. Schofield, *Tetrahedron Lett.* **1962**, *3*, 697–699.
[41] D. H. R. Barton, Y. L. Chow, A. Cox, G. W. Kirby, *Tetrahedron Lett.* **1962**, *3*, 1055–1057.
[42] D. H. R. Barton, Y. L. Chow, A. Cox, G. W. Kirby, *J. Chem. Soc. Resumed* **1965**, 3571–3578.
[43] A. Patchornik, B. Amit, R. B. Woodward, *J. Am. Chem. Soc.* **1970**, *92*, 6333–6335.
[44] J. H. Kaplan, B. I. Forbush, J. F. Hoffman, *Biochemistry* **1978**, *17*, 1929–1935.
[45] J. Engels, E. J. Schlaeger, *J. Med. Chem.* **1977**, *20*, 907–911.
[46] V. B. Kammath, P. Šebej, T. Slanina, Z. Kříž, P. Klán, *Photochem Photobiol Sci* **2012**, *11*, 500–507.
[47] T. Slanina, P. Šebej, A. Heckel, R. S. Givens, P. Klán, *Org. Lett.* **2015**, *17*, 4814–4817.
[48] R. S. Givens, A. Jung, C. H. Park, J. Weber, W. Bartlett, *J. Am. Chem. Soc.* **1997**, *119*, 8369–8370.
[49] B. P. Ngoy, P. Šebej, T. Šolomek, B. H. Lim, T. Pastierik, B. S. Park, R. S. Givens, D. Heger, P. Klán, *Photochem. Photobiol. Sci.* **2012**, *11*, 1465–1475.
[50] P. G. Conrad, R. S. Givens, B. Hellrung, C. S. Rajesh, M. Ramseier, J. Wirz, *J. Am. Chem. Soc.* **2000**, *122*, 9346–9347.
[51] M. Reinfelds, J. von Cosel, K. Falahati, C. Hamerla, T. Slanina, I. Burghardt, A. Heckel, *Chem. – Eur. J.* **2018**, *24*, 13026–13035.
[52] P. Šebej, J. Wintner, P. Müller, T. Slanina, J. Al Anshori, L. A. P. Antony, P. Klán, J. Wirz, *J. Org. Chem.* **2013**, *78*, 1833–1843.
[53] H. E. Zimmerman, V. R. Sandel, *J. Am. Chem. Soc.* **1963**, *85*, 915–922.
[54] T. Šolomek, J. Wirz, P. Klán, *Acc. Chem. Res.* **2015**, *48*, 3064–3072.
[55] M. Martínek, J. Váňa, P. Šebej, R. Navrátil, T. Slanina, L. Ludvíková, J. Roithová, P. Klán, *ChemPlusChem* **2020**, *85*, 2230–2242.
[56] A. Poryvai, M. Galkin, V. Shvadchak, T. Slanina, *Angew. Chem. Int. Ed.* **2022**, *61*, e202205855.
[57] P. Štacko, P. Šebej, A. T. Veetil, P. Klán, *Org. Lett.* **2012**, *14*, 4918–4921.
[58] Y.-R. Luo, *Comprehensive Handbook of Chemical Bond Energies*, CRC Press, Boca Raton, **2007**.
[59] A. P. Demchenko, *Methods Appl. Fluoresc.* **2020**, *8*, 022001.
[60] P. P. Goswami, A. Syed, C. L. Beck, T. R. Albright, K. M. Mahoney, R. Unash, E. A. Smith, A. H. Winter, *J. Am. Chem. Soc.* **2015**, *137*, 3783–3786.
[61] N. Rubinstein, P. Liu, E. W. Miller, R. Weinstain, *Chem Commun* **2015**, *51*, 6369–6372.
[62] J. V. Frangioni, *Curr. Opin. Chem. Biol.* **2003**, *7*, 626–634.
[63] R. Weissleder, *Nat. Biotechnol.* **2001**, *19*, 316–317.
[64] S. J. Jang, *J. Chem. Phys.* **2021**, *155*, 164106.
[65] L. A. P. Antony, T. Slanina, P. Šebej, T. Šolomek, P. Klán, *Org. Lett.* **2013**, *15*, 4552–4555.
[66] E. Palao, T. Slanina, L. Muchova, T. Solomek, L. Vitek, P. Klan, *J. Am. Chem. Soc.* **2016**, *138*, 126–133.

[67] T. Slanina, P. Šebej, *Photochem. Photobiol. Sci.* **2018**, *17*, 692–710.
[68] L. Wohlrábová, J. Okoročenkova, E. Palao, E. Kužmová, K. Chalupský, P. Klán, T. Slanina, *Org. Lett.* **2023**, *25*, 6705–6709.
[69] P. Jedináková, P. Šebej, T. Slanina, P. Klán, J. Hlaváč, *Chem Commun* **2016**, *52*, 4792–4795.
[70] D. Madea, T. Slanina, P. Klán, *Chem Commun* **2016**, *52*, 12901–12904.
[71] H. C. Kolb, M. G. Finn, K. B. Sharpless, *Angew. Chem. Int. Ed.* **2001**, *40*, 2004–2021.
[72] P. Shieh, M. R. Hill, W. Zhang, S. L. Kristufek, J. A. Johnson, *Chem. Rev.* **2021**, DOI 10.1021/acs.chemrev.0c01282.
[73] M. Reinfelds, V. Hermanns, T. Halbritter, J. Wachtveitl, M. Braun, T. Slanina, A. Heckel, *ChemPhotoChem* **2019**, *3*, 441–449.
[74] L. Čechová, J. Filo, M. Dračínský, C. Slavov, D. Sun, Z. Janeba, T. Slanina, J. Wachtveitl, E. Procházková, M. Cigáň, *Angew. Chem. Int. Ed.* **2020**, *59*, 15590–15594.
[75] A. K. Gaur, D. Gupta, A. Mahadevan, P. Kumar, H. Kumar, D. N. Nampoothiry, N. Kaur, S. K. Thakur, S. Singh, T. Slanina, S. Venkataramani, *J. Am. Chem. Soc.* **2023**, *145*, 10584–10594.
[76] A. Goulet-Hanssens, F. Eisenreich, S. Hecht, *Adv. Mater.* **2020**, *32*, 1905966.
[77] G. C. Thaggard, J. Haimerl, K. C. Park, J. Lim, R. A. Fischer, B. K. P. Maldeni Kankanamalage, B. J. Yarbrough, G. R. Wilson, N. B. Shustova, *J. Am. Chem. Soc.* **2022**, *144*, 23249–23263.
[78] K. Hüll, J. Morstein, D. Trauner, *Chem. Rev.* **2018**, *118*, 10710–10747.
[79] M.-M. Russew, S. Hecht, *Adv. Mater.* **2010**, *22*, 3348–3360.
[80] T. I. U. of P. and A. Chemistry (IUPAC), "IUPAC - Gibbs energy of photoinduced electron transfer (GT07388)," DOI 10.1351/goldbook.GT07388can be found under https://goldbook.iupac.org/terms/view/GT07388, **n.d.**
[81] B. Saxena, R. I. Patel, A. Sharma, *Adv. Synth. Catal.* **2023**, *365*, 1538–1564.
[82] J. R. Štoček, O. Socha, I. Císařová, T. Slanina, M. Dračínský, *J. Am. Chem. Soc.* **2022**, *144*, 7111–7116.
[83] T. Nemirovich, V. Kostal, J. Copko, H. C. Schewe, S. Boháčová, T. Martinek, T. Slanina, P. Jungwirth, *J. Am. Chem. Soc.* **2022**, *144*, 22093–22100.
[84] E. Zurek, P. P. Edwards, R. Hoffmann, *Angew. Chem. Int. Ed.* **2009**, *48*, 8198–8232.
[85] S. J. M. Thomas, P. P. Edwards, V. L. Kuznetsov, *ChemPhysChem* **2008**, *9*, 59–66.
[86] A. J. Birch, *Nature* **1946**, *158*, 585–585.
[87] T. Fiala, L. Ludvíková, D. Heger, J. Švec, T. Slanina, L. Vetráková, M. Babiak, M. Nečas, P. Kulhánek, P. Klán, V. Sindelar, *J. Am. Chem. Soc.* **2017**, *139*, 2597–2603.
[88] T. Slanina, T. Oberschmid, *ChemCatChem* **2018**, *10*, 4182–4190.
[89] B. Schlemmer, A. Sauermoser, S. Holler, E. Zuccalà, B. Ehmann, M. Reinfelds, R. C. Fischer, H. Amenitsch, J. M. Marin-Beloqui, L. Ludvíková, T. Slanina, M. Haas, T. Rath, G. Trimmel, *Chem. – Eur. J.* **2023**, *29*, e202301337.
[90] I. Ghosh, B. König, *Angew. Chem. Int. Ed.* **2016**, *55*, 7676–7679.
[91] D. Hidasová, T. Slanina, *J. Org. Chem.* **2023**, acs.joc.3c00238.
[92] D. Hernández-Guerra, A. Hlavačková, C. Pramthaisong, I. Vespoli, R. Pohl, T. Slanina, U. Jahn, *Angew. Chem. Int. Ed.* **2019**, *58*, 12440–12445.
[93] K. Rahimidashaghoul, I. Klimánková, M. Hubálek, V. Matoušek, J. Filgas, P. Slavíček, T. Slanina, P. Beier, *ChemPhotoChem* **2021**, *5*, 43–50.
[94] M. Melchionna, P. Fornasiero, *ACS Catal.* **2020**, *10*, 5493–5501.
[95] N. A. Romero, D. A. Nicewicz, *Chem. Rev.* **2016**, *116*, 10075–10166.
[96] A. U. Meyer, K. Straková, T. Slanina, B. König, *Chem. - Eur. J.* **2016**, *22*, 8694–8699.
[97] T. Ghosh, T. Slanina, B. König, *Chem Sci* **2015**, *6*, 2027–2034.
[98] A. U. Meyer, T. Slanina, A. Heckel, B. König, *Chem. – Eur. J.* **2017**, *23*, 7900–7904.

[99] I. Ghosh, T. Ghosh, J. I. Bardagi, B. Konig, *Science* **2014**, *346*, 725–728.
[100] T. Hering, T. Slanina, A. Hancock, U. Wille, B. König, *Chem Commun* **2015**, *51*, 6568–6571.
[101] R. Obertík, J. Chudoba, J. Šturala, J. Tarábek, L. Ludvíková, T. Slanina, B. König, R. Cibulka, *Chem. – Eur. J.* **2022**, *28*, e202202487.
[102] A. U. Meyer, T. Slanina, C.-J. Yao, B. König, *ACS Catal.* **2016**, *6*, 369–375.
[103] V. Mojr, G. Pitrová, K. Straková, D. Prukała, S. Brazevic, E. Svobodová, I. Hoskovcová, G. Burdziński, T. Slanina, M. Sikorski, R. Cibulka, *ChemCatChem* **2018**, *10*, 849–858.
[104] J. Žurauskas, S. Boháčová, S. Wu, V. Butera, S. Schmid, M. Domański, T. Slanina, J. P. Barham, *Angew. Chem. Int. Ed.* **2023**, *62*, e202307550.

Attached Publications

List of selected research publications

1. *J. Am. Chem. Soc.* **2020**, 142, 10942-10954: benzene rearrangement
2. *J. Am. Chem. Soc.* **2023**, 145, 21569-21575: azulene properties
3. *Cell Rep. Phys. Sci.* **2020**, 1, 100274: photodegradation of amiloride
4. *Photochem. Photobiol. Sci*. **2016**, 15, 250-259: chalcogen monosubstituted BODIPY
5. *Chem. Commun*. **2016**, 52, 11951-11954: chalcogen disubstituted BODIPY
6. *Chem. Commun*. **2022**, 55, 6389: chalcogen BODIPY sensors for enzymes
7. *Photochem. Photobiol. Sci*. **2012**, 11, 500-507: photoremovable chiral auxiliary
8. *Org. Lett.* **2015**, 17, 4814–4817: photocaged fluoride
9. *Chem. Eur. J.* **2018**, 24, 13026-13035: meta effect-based photocages
10. *J. Org. Chem.* **2013**, 78, 1833-1843: fluorescein-based photocage
11. *J. Am. Chem. Soc.* **2017**, 139, 15168-15175: meso-methyl BODIPY photocage
12. *ChemPlusChem* **2020**, 85, 2230-2242: 1,3-dithianyl pyronin photocage
13. *Angew. Chem. Int. Ed.* **2022**, e202205855: extended BODIPY photocages for oleic acid
14. *Org. Lett.* **2013**, 15, 4552–4555: xanthene-based photoCORMs
15. *J. Am. Chem. Soc.* **2016**, 138, 126-133: BODIPY-based photoCORM
16. *Org. Lett.* **2023**, 25, 6705-6709: H_2S_n photorelease from BODIPY cages
17. *Chem. Commun.* **2016**, 52, 4792 – 4795: photoclick using selenadiazoles
18. *Chem. Commun.* **2016**, 52, 12901-12904: catch and release system
19. *ChemPhotoChem*, **2019**, 3, 441-449: fulgide actinometer
20. *J. Am. Chem. Soc.* **2023**, 10584: bistable heteroazoarenes
21. *Angew. Chem. Int. Ed.* **2020**, 59, 15590-15594: 5-phenylazopyrimidines ultrafast oscillators
22. *J. Am. Chem. Soc.* **2022**, 144, 7111: salt or cocrystal?
23. *J. Am. Chem. Soc.* **2022**, 144, 22093: solvated electrons in ammonia
24. *J. Am. Chem. Soc.* **2017**, 139, 2597-2603: stable radical cation of methyl viologen
25. *ChemCatChem*, **2018**, 18, 4182-4190: rhodamine 6G radical
26. *Chem. Eur. J.* **2023**, 29, e202301337: Ge and Si-substituted PDI for solar cells
27. *J. Org. Chem.* **2023**, 6932: magic blue reactivity
28. *Angew. Chem. Int. Ed.* **2019**, 58, 12440-12445: photochemical C-H amination
29. *ChemPhotoChem* **2021**, 5, 43-50: photochemical fluoroalkylation
30. *Chem. Sci.* **2015**, 6, 2027-2034: photocatalytic aldehyde reduction
31. *Chem. Eur. J.* **2017**, 23, 7900-7904: photocatalytic dehalogenations using lanthanide salts
32. *Chem. Commun.* **2015**, 51, 6568-6571: photocatalytic nitrate radical generation
33. *Chem. Eur. J.* **2022**, e202202487: chemoselective photooxidations
34. *ACS Catal.* **2016**, 6, 369-375: photocatalytic perfluoroarylation
35. *Chem. Eur. J.* **2016**, 22, 8694–8699: photocatalytic sulfonylation
36. *ChemCatChem* **2018**, 10, 849-858: photocatalytic cycloadditions
37. *Angew. Chem. Int. Ed.* **2023**, 62, e202307550: acridones and acridinia for arylation